

# Grid cells and cortical representation

Edvard I. Moser<sup>1</sup>, Yasser Roudi<sup>1</sup>, Menno P. Witter<sup>1</sup>, Clifford Kentros<sup>1,2</sup>, Tobias Bonhoeffer<sup>1,3</sup> and May-Britt Moser<sup>1</sup>

**Abstract** | One of the grand challenges in neuroscience is to comprehend neural computation in the association cortices, the parts of the cortex that have shown the largest expansion and differentiation during mammalian evolution and that are thought to contribute profoundly to the emergence of advanced cognition in humans. In this Review, we use grid cells in the medial entorhinal cortex as a gateway to understand network computation at a stage of cortical processing in which firing patterns are shaped not primarily by incoming sensory signals but to a large extent by the intrinsic properties of the local circuit.

## Entorhinal cortex

An interface between the three-layered hippocampal cortex and six-layered neocortex. It provides the main cortical input to the dentate gyrus.

## Place cell

A type of hippocampal neuron that typically has a single environmentally specific spatial receptive field. There is no discernible relationship between firing patterns in different environments.

*Idealists argue that the hexagonal rooms are the necessary shape of absolute space, or at least of our perception of space. The Library of Babel, Jorge Luis Borges*

The nervous system has evolved to enable adaptive decision making and behaviour in response to changes in the internal and external environment. To permit adaptive responses, nervous systems recreate properties of the internal or external world in activity patterns that are referred to as neural representations. Representations can be thought of as dynamic clusters of cells, the activity patterns of which correlate with features of the outside world. By recreating the environment in a language that is suitable for brain computation, representations are thought to mediate the selection of appropriate action in response to stimulus configurations in the animal's environment. Given the importance of internal representations in guiding behaviour, understanding their mechanisms has become one of the central goals of contemporary neuroscience.

Representations have been studied at multiple levels, from the earliest stages of sensory systems, where sensory maps reproduce the spatial organization of the sensory receptors, to the highest levels of association cortices, where representations bear little resemblance to activation patterns in the receptor population (BOX 1). The mechanisms underlying the formation of representations at the bottom of the representational hierarchy (near the sensory receptor populations) have been explored extensively, particularly in the visual system. Much less is known about how representations form at higher levels, where representations depend more strongly on intrinsic cortical computations. The aim of this Review is to discuss mechanisms of neural

representation in the medial entorhinal cortex (MEC), which is near the apex of the cortical hierarchy<sup>1</sup>, using well-studied representations in the primary visual cortex (V1) as a reference.

## Place cells and grid cells

The MEC and the hippocampus are a part of the brain's neural map of external space<sup>2–4</sup> (BOX 2). Multiple functional cell types contribute to this representation. The first spatial cell type to be discovered was the place cell<sup>5,6</sup>. Place cells are hippocampal cells that fire selectively when animals are at certain locations in the environment. The description of place cells in the 1970s was followed, more than 30 years later, by the discovery of grid cells, one synapse upstream of place cells, in the MEC<sup>7–9</sup>. Grid cells are place-selective cells that fire at multiple discrete and regularly spaced locations<sup>7</sup>. These firing locations form a hexagonal pattern that tiles the entire space that is available to the animal<sup>8</sup> (FIG. 1a). Whereas ensembles of place cells change unpredictably from one environment to the next<sup>10,11</sup>, the positional relationship between grid cells is maintained, reflecting the structure of space independently of the contextual details of individual environments<sup>12</sup>. The rigid structure of the grid map, along with its spatial periodicity, points to grid cells as a part of the brain's metric for local space<sup>4,12</sup>.

Place cells and grid cells were discovered in rats, but similar cells have subsequently been reported in mice<sup>13–15</sup>, bats<sup>16,17</sup>, monkeys<sup>18–21</sup> and humans<sup>22,23</sup>, although the bulk of research on entorhinal–hippocampal spatial representation is still carried out using rodents. The strong correspondence in each species between entorhinal–hippocampal firing patterns and a measurable property of the external world — the location of

<sup>1</sup>Kavli Institute for Systems Neuroscience and Centre for Neural Computation,

Norwegian University of Science and Technology, 7491 Trondheim, Norway.

<sup>2</sup>Institute of Neuroscience, University of Oregon, Eugene, Oregon 97403-1254, USA.

<sup>3</sup>Max Planck Institute of Neurobiology, Am Klopferspitz 18, 82152 Planegg-Martinsried, Germany.

Correspondence to E.I.M. e-mail: [edvard.moser@ntnu.no](mailto:edvard.moser@ntnu.no)

doi:10.1038/nrn3766

Published online

11 June 2014

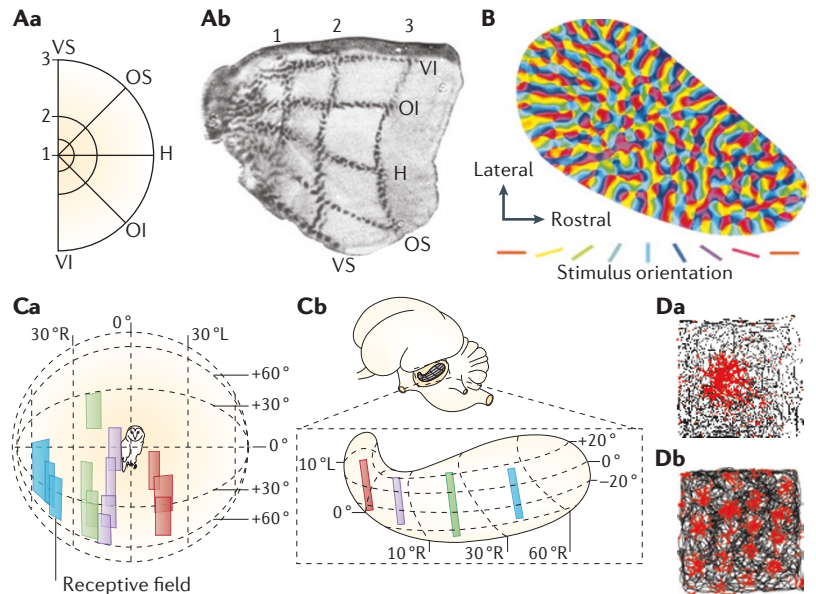
the animal — makes the spatial representation circuit a powerful experimental model system for understanding neural computation at the highest levels of the association cortices, many synapses away from sensory receptors and motor outputs.

**Grid cells and sensory inputs**

The defining feature of grid cells is their hexagonal firing structure<sup>8</sup>. However, grid cells differ in grid spacing (the distance between grid fields), grid orientation (the rotation of grid axes) and grid phase (the *x-y* locations

**Box 1 | Hierarchy of cortical representation**

Mechanisms of neuronal representation have been explored at several levels. The simplest representations are found at early stages of sensory systems, where the outside world is reproduced in the form of orderly maps that reflect the spatial organization of the sensory receptors. The retinotopic maps of the optic tectum<sup>180</sup> and the visual cortex<sup>64,66</sup>, the body-surface representations of the somatosensory cortex<sup>181,182</sup> and the tonotopic maps of the auditory cortex<sup>183,184</sup> are examples of such representations, in which a distorted but neighbourhood-preserving projection is formed between the sensory organ and the brain.



Panel **A** of the figure illustrates the retinotopic organization of the macaque visual cortex<sup>66</sup>. The visual stimulus used in this experiment is illustrated in panel **Aa**. Panel **Ab** shows a tangential autoradiograph of the primary visual cortex (V1) layer 4C after presentation of the visual stimulus with its centre on the fovea. The fovea is represented to the left, and the periphery to the right (VS and VI, vertical superior and inferior rays of the stimulus; OS and OI, oblique superior and inferior rays; H, horizontal meridian; numbers indicate first, second and third ring of the stimulus). Note that the stimulus (or the spatial organization of the sensory receptors) is reproduced as an orderly map on the cortical surface.

The orientation maps in the visual systems of many higher mammals are examples of a more complex level of cortical representation<sup>43,61–63,185,186</sup>, in which orientation-selective simple cells are thought to be built by combining information from multiple ganglion cells, the receptive fields of which are slightly offset along one axis in visual space<sup>156,187</sup>. Panel **B** of the figure shows an orientation preference map (surface view) of tree shrew V1; the orientation of a square-wave grating stimulus is colour-coded, as indicated at the bottom<sup>114</sup>. Orientation maps require a wiring scheme by which strict neighbourhood relationships in the projection between the sensory organ and target neurons are lost. Building and maintaining this connectivity is a formidable task, but an orderly representation of parameters that are important for further cortical processing seems to be advantageous for the brain. Higher levels of the visual system feature cells that respond to sophisticated combinations of size, shape, colour, orientation and direction<sup>188–190</sup>, and even to ethologically important objects, including hands and individual faces<sup>189,191–197</sup>.

At a third level of complexity, maps are no longer generated by simple geometrical transformations between the receptor surface and the target brain structure. An example is the ‘computational map’ of auditory space in the inferior colliculus of the barn owl, in which time and amplitude differences between signals from the two ears are used to compute the location of a sound source<sup>198,199</sup>. Panel **Ca** of the figure illustrates coordinates of auditory space around the owl (the globe shape indicated by the dashed lines)<sup>198</sup>. Receptive field locations are projected onto the globe for 14 neurons (which are represented by coloured rectangles; different electrode penetrations in the midbrain auditory area have different colours). The top part of panel **Cb** shows the location of the barn owl midbrain auditory area and the bottom part shows a schematic section through this area with isoazimuth and isoelevation contours based on receptive field centres, as shown in panel **Ca**. Receptive field locations are colour-coded. Note topographic mapping of auditory space in two dimensions.

At the very peak of the hierarchy, the structure of the representation is thought to depend strongly on intrinsic circuit mechanisms. The most extensively studied example of such non-topographic representation is the map of external space in the hippocampus and the medial entorhinal cortex, with place cells<sup>5</sup> and grid cells<sup>8</sup>, respectively, as principal functional cell types. Part **Da** of the figure shows the firing-rate map of a place cell, and part **Db** shows the firing-rate map of a grid cell. These firing patterns are unique in that they no longer reflect stimulus configurations in the external world but largely represent pattern formation processes within entorhinal–hippocampal local circuits.

Part **A** adapted with permission from REF. 66, Society for Neuroscience. Part **B** reprinted with permission from REF. 114, Society for Neuroscience. Part **C** is from Knudsen, E. I. & Konishi, M. A neural map of auditory space in the owl. *Science* **200**, 795–797 (1978). Reprinted with permission from AAAS.

**Grid cells**

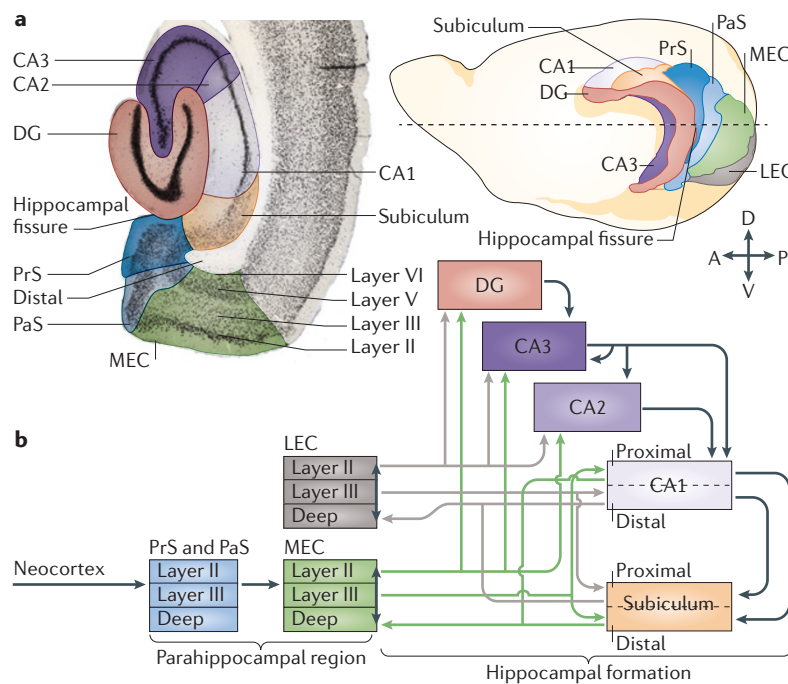
Parahippocampal neurons that have regularly repeating hexagonally spaced receptive fields. Co-activity patterns remain largely the same across different environments.

**Box 2 | Anatomy of hippocampal formation and parahippocampal region**

One of the principal features of the cortex is its layered organization. The cortex has essentially two forms, the neocortex (also called the isocortex), which is generally thought to comprise five or six layers, and the allocortex, which is characterized by three layers. In between these two types, several transition areas have been recognized, where the number of layers increases from three to six. The entorhinal cortex together with the presubiculum (PrS) and parasubiculum (PaS) are parts of this transition domain.

Part **a** of the figure shows the right hemisphere of a rat brain, with a focus on the hippocampal formation and the parahippocampal region. The left part is a horizontal section through the hemisphere; the right part shows a mid-sagittal view of the hemisphere, based on the rat Waxholm space<sup>200</sup>. The dorsoventral position of the section is indicated by the dashed line through the hemisphere. Together, the images illustrate the positions of key hippocampal and parahippocampal areas: the dentate gyrus (DG), CA1–CA3, the subiculum, the medial entorhinal cortex (MEC), the lateral entorhinal cortex (LEC), the PrS and the PaS. The borders and the extent of individual subregions are colour-coded.

In the current standard connectivity model of the hippocampal formation and parahippocampal region (see the figure, part **b**), the MEC provides input to the hippocampal formation, with layer II projecting to the DG, CA3 and CA2, and layer III projecting to CA1 and the subiculum. CA1 and the subiculum provide output to entorhinal cortex layer V. All entorhinal layers seem to be reciprocally connected (indicated by the double-headed arrows). This connectional route, in green, is paralleled by a similarly organized route starting and ending in the LEC, indicated in grey. The two pathways converge onto single neurons in the DG, CA3 and CA2 but target different neurons in CA1 and the subiculum. Projections from and to the MEC link to neurons in CA1 close to CA2 (proximal) and neurons in the subiculum close to the PrS (distal), and the opposite pattern holds for projections from and to the LEC. Inputs selective for the MEC originate from the PrS and the PaS.



A, anterior; D, dorsal; P, posterior; V, ventral.

of firing vertices)<sup>8,24</sup> (FIG. 1 b). Grid cells exhibit variable degrees of asymmetry<sup>24,25</sup>, and periodicity may be expressed more strongly along one axis of the triangular grid than the two others<sup>26</sup>. Collectively, the variety of grid cells defines a map of the animal's relative position in the environment<sup>7,12</sup>. Because grid cells differ in spacing,

each place in the local environment is associated with a unique combination of active cells, enabling neurons with access to this combined activity to faithfully read out the animal's location.

The map of grid cells is dynamic, in the sense that activation is driven by the animal's movement in the environment<sup>3,8</sup>. For grid activity to be updated in accordance with ongoing movement, grid cells must have access to sensory signals that correspond to the animal's change in location. Only a few types of sensory input are sufficiently continuous to enable smooth translation of the grid representation. Such inputs include proprioceptive and kinaesthetic feedback as well as vestibular signals and optic flow. Consistent with a primary role for self-motion inputs and a secondary role for inputs from stationary cues, grid cells retain their hexagonal firing pattern after removal of visual or olfactory landmarks<sup>8,12</sup>. Pairs of grid cells tend to maintain spatial firing relationships across environments, independently of landmark identities<sup>12</sup>, as expected if the algorithm were based on self-motion.

A strong dependence on motion cues might imply a role for grid cells in representations based on path integration, a process whereby animals keep track of their position by integrating linear and angular running speed over time to yield spatial displacement relative to a reference position (for example, the starting position of a path)<sup>27–29</sup>. Both place cells and grid cells express outcomes of path integration, in the sense that firing fields can often be related to distance of movement from a reference position rather than to inputs from stationary visual cues<sup>30–34</sup>. Recent work has identified a dedicated cell population for linear representation of running speed within the MEC<sup>35</sup>. By integrating speed over time, these speed cells may provide grid cells with information about changes in position. A role for speed cells and grid cells in path integration is consistent with the observation that rats with MEC lesions fail to navigate back to a refuge under conditions in which only self-motion cues are informative<sup>36,37</sup>. However, mechanisms for path integration may exist in multiple brain circuits, as suggested by the fact that, in humans, unlike rats, simple self-motion-based navigation is spared by lesions that include the entorhinal cortex<sup>37,38</sup>.

Path integration can only be used to calculate displacement from fixed reference positions. Stationary cues are required to associate path-integration coordinates with absolute position. The fact that grid phase and grid orientation remain stable across test sessions<sup>8</sup>, and that grid fields rotate along with external reference points in cylindrical environments<sup>8</sup>, suggests that grid coordinates are anchored to the external environment. Experiments in compartmentalized mazes suggest that grid maps anchor at many locations and often near salient environmental features<sup>32</sup>. Frequent anchoring may prevent drift owing to accumulation of path-integration error<sup>39</sup>. However, the frequency at which grid maps are updated is not known. Grid maps may be re-anchored at regular intervals — for example, on individual cycles of the local theta rhythm — or resetting may occur in response to specific cues in the environment.

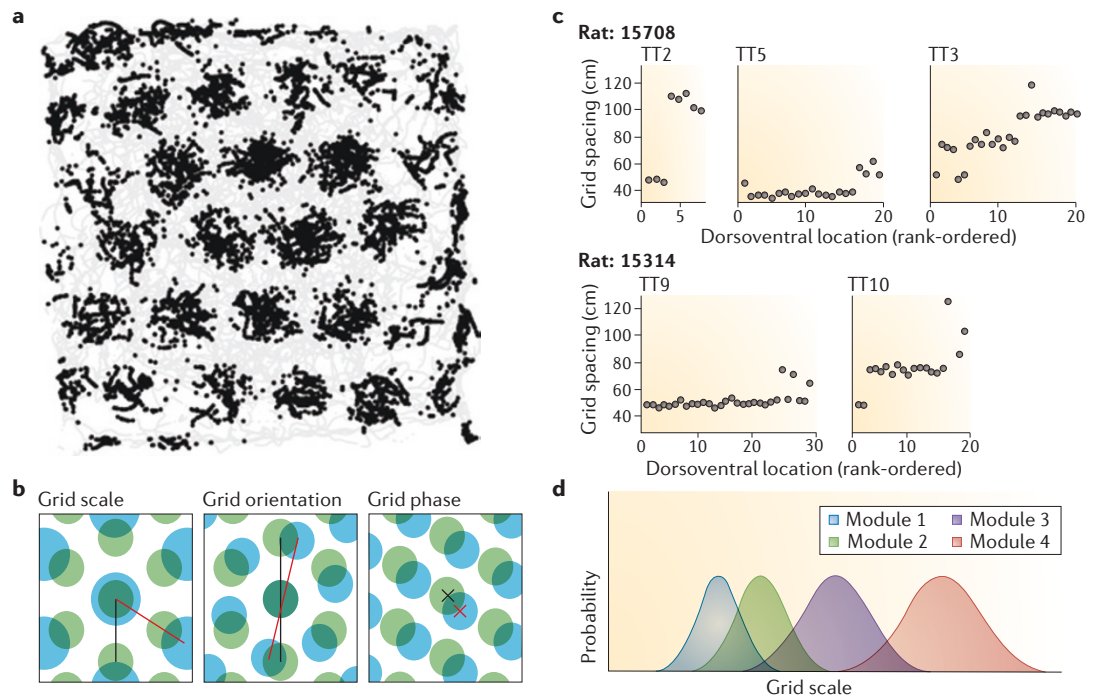


**Figure 1 | Basic properties of grid cells.** **a** | Spatial firing pattern of a grid cell from layer II of the rat medial entorhinal cortex (MEC). The grey trace shows the trajectory of a foraging rat in a 2.2 m wide square enclosure. The locations at which the grid cell spikes are superimposed on the trajectory are shown in black. Each black dot corresponds to one spike. Note the periodic hexagonal pattern of the firing fields of the grid cell. **b** | Cartoons of firing patterns of pairs of grid cells (shown in blue and green), illustrating the differences between grid scale, grid orientation and grid phase. Lines in left and middle panels indicate two axes of the grid pattern (which define grid orientation); crosses in the panel on the right indicate grid phase ( $x$ - $y$  location of grid fields). **c** | Modular organization of the grid scale. Grid spacing is shown as a function of position along the recording track in the MEC, with cells (represented by grey circles) rank-ordered from dorsal to ventral and one panel per tetrode (TT). On each tetrode, grid spacing increases in discrete steps. **d** | A schematic showing that the increase in grid scale across modules follows a geometric progression rule. From one module to the next, average grid scale increases by a constant factor (1.4 in this case). Part **a** is reprinted from Moser, E. I. & Moser, M. B. Grid cells and neural coding in high-end cortices. *Neuron* **80**, 765–774 (2013)<sup>229</sup>. Copyright (2013), with permission from Elsevier. Part **c** from REF. 24, Nature Publishing Group.

**Architecture of the grid map**

Although grid fields are modulated by sensory inputs, such inputs are not sufficient to explain how the grid pattern itself is formed. The hexagonal grid pattern is not reflected in any of the polysynaptic sensory inputs to the grid cells, suggesting that it arises intrinsically in the MEC or the wider parahippocampal circuit of which the MEC is a part. This possibility justifies a closer look at the functional architecture of the grid cell network.

The organization of grid cells is partly topographic and partly non-topographic<sup>8</sup>. Grid scale shows topographic organization in the sense that grid cells with small fields and small interfield distances predominate in the dorsal part of the MEC. At more ventral levels, cells with larger grid scales predominate<sup>7,24,40</sup>. By contrast, the phase of the grid pattern exhibits no discernible large-scale topography<sup>8</sup>. Local ensembles of grid cells apparently cover the entire range of grid phases at all MEC locations. The distribution of grid phases is similar to the interspersed or salt-and-pepper-like organization of response properties in several sensory cortices, such as odour representations in the piriform cortex<sup>41,42</sup> or orientation maps in the visual cortex of rodents<sup>43–45</sup>.

However, fine-scale topography of grid phase has not been ruled out. Samples of simultaneously recorded cells are generally small, and the resolution of tetrode recordings does not enable anatomical mapping at a scale of less than 50–100 micrometres<sup>46</sup>. Thus, approaches with better anatomical resolution need to be developed before estimates of the functional microarchitecture can be made<sup>47,48</sup>.

The lack of grid-phase topography does not rule out the presence of discrete cell assemblies with unique functions. Recent recordings from up to almost 200 grid cells per animal have suggested, in agreement with a small sample of data from an earlier study<sup>25</sup>, that grid cells cluster into modules of cells with similar grid scale, grid orientation and grid asymmetry but different grid phase<sup>24</sup> (FIG. 1c). Modules with short grid wavelengths (spacing) predominate at the dorsal end of the MEC. Larger-scale modules are added successively towards the ventral MEC without discarding the shorter wavelengths. The increase in grid scale is discontinuous. If grid modules are sorted by wavelength, from short to long, the average wavelength increases from one module to the next by a factor of 1.4, as in a geometric progression (FIG. 1d). At the same time, the number of cells per module decreases.

**Theta rhythm**

Oscillatory activity in the range of 6–10 Hz in the local field potential of the hippocampus. It is produced by large and widespread ensembles of hippocampal neurons that oscillate in synchrony.

**Salt-and-pepper-like organization**

Cortical architecture in which single cells are tuned for the orientation of a stimulus but show no particular order in their arrangement. This arrangement is seen in the rodent visual cortex.

Theoretical analyses suggest that such an organization may be optimal for obtaining maximal spatial resolution from a minimal number of grid cells<sup>49,50</sup>. The emergence of an architecture that maximizes information from a limited pool of neurons is reminiscent of the balance between the number of on and off cells in the retina, which has been shown to match the statistical structure of common visual scenes<sup>51</sup>.

The functional coherence of grid cells within modules and their separation from grid cells in other modules raise the possibility that grid networks consist of anatomically overlapping subnetworks that exhibit strong intrinsic coupling but weaker coupling to other subnetworks. Key questions for the future will be to determine which cells wire together in such networks, at which developmental stage this wiring takes place and how cells of the same network find each other. For functional maps in the visual cortex, there is more information on these questions: it is now reasonably well established that activity-dependent mechanisms are involved in forming the map or, in the special case of rodents, connecting cells with particular response properties<sup>52–54</sup>. The basic organization of connections in the visual pathway is established before visual experience as a result of spontaneous correlated activity (retinal and cortical waves)<sup>55–58</sup> or by means of gap-junction coupling of clonally related neurons at prenatal developmental stages<sup>59,60</sup>. It remains unknown whether the developmental processes underlying the modular architecture of grid cell ensembles rely on similar mechanisms.

The entangled nature of grid modules differs from the organization of representations for continuous variables in some other cortical systems. For example, in the visual cortex of cats and monkeys, orientation-selective cells are organized into continuous pinwheel-like structures that map orientations successively through the 180-degree orientation cycle<sup>61</sup>. Orientation maps in these species are smooth except at the very centre of the pinwheel<sup>62,63</sup> and at the border between direction-sensitive domains<sup>43</sup>. Because orientation is circular, a pinwheel-like arrangement may be required for optimal continuity. Other parameters such as ocular dominance, disparity, spatial frequency and, of course, position in space are mapped continuously across the entire cortical surface<sup>64–70</sup>. A notable exception is the salt-and-pepper-like organization of orientation tuning in the rodent visual cortex<sup>43–45</sup>. Plausible explanations for this exception lie in the relative scale of the cortical area, the magnification factor and the receptive field scatter, which make an interspersed organization a necessity if all stimulus parameters are to be represented in each region of visual space. If a mouse had functional columns the size of those in cats, and not a salt-and-pepper-like organization, it would only see one stimulus feature — for example, one orientation — in any portion of the visual field. We can only speculate whether a similar explanation may hold true for the salt-and-pepper-like representation of grid phase in the MEC, whether grid phase would be represented topographically in mammals with larger MECs and whether topographic representation matters for the way animals perceive space.

Finally, MEC networks do not only consist of grid cells. Grid cells intermingle with head direction cells — cells that fire only if the rat's head is pointing in a certain direction relative to external cues. These cells were first found in the adjacent presubiculum<sup>71,72</sup> but were subsequently also recorded in the MEC<sup>9</sup>. Grid cells and head direction cells further intermingle with border cells — cells that fire exclusively when the rat is close to a salient border of the environment, such as the wall of a recording enclosure or the edge of a platform<sup>73,74</sup> — as well as the aforementioned speed cells, the firing rates of which increase monotonically with running speed, independently of the rat's location or head direction<sup>35</sup>. Cells with border-determined firing properties also exist in the subiculum<sup>75,76</sup>. Grid cells, head direction cells, border cells and speed cells are functionally discrete populations but coexist with cells with conjunctive properties<sup>9,35,74</sup>. The mixture of functional cell types in the MEC has an interesting analogy in the visual system in visual area V2 — and to a lesser extent V1 — where, at least in primates, cells coding for colour, disparity, orientation, motion, spatial frequency and other properties coexist, albeit to a certain extent in certain compartments<sup>77</sup>. In the visual cortex, as in the MEC, functional properties are distributed onto discrete but intermingled cell types.

### Attractor networks and mechanisms

Several properties of grid cells point to local circuit computation as the source of the grid pattern. Within modules of grid cells, cell assemblies respond with coherent changes in grid phase, grid orientation and grid scale when the animal is brought to a different environment<sup>12,24</sup> or following interventions that change the scale of the grid, such as exposure to an unfamiliar environment<sup>25,78,79</sup> or compression of the recording enclosure<sup>24,25</sup>. In each case, the relationship between firing fields of cell pairs is conserved despite major changes in the properties of individual cells and without any obvious relationship to sensory inputs<sup>78</sup>. These observations are consistent with the idea that grid cells operate as ensembles of interconnected neurons whose activity patterns move across continua of attractor states (BOX 3; FIG. 2). Attractor models provide powerful working hypotheses for grid cells, although alternative mechanisms, such as interference between theta-frequency membrane potential oscillations<sup>80–82</sup>, have also been explored<sup>4,83</sup>. Oscillatory interference models of grid cells have guided some of the most important experimental studies on grid cells, but there is mounting experimental evidence against simple versions of these models (BOX 4). The focus of this article is therefore on attractor network-based mechanisms.

The idea of an attractor network is one of the most influential concepts in theoretical systems neuroscience<sup>84–87</sup>. Attractor networks can be traced back to Donald Hebb<sup>88</sup> who argued that co-firing neurons should be more strongly connected to each other than to the rest of the network, thus forming so-called Hebbian cell assemblies. Activating a subset of the neurons in such an assembly will lead to activation of the rest. The

#### Head direction cells

Neurons found throughout parahippocampal areas and in other brain regions (for example, the anterior thalamus) for which the primary feature of the receptive field is the direction in which the animal's head is pointing.

#### Attractor network

A network with one or more stable firing-rate pattern that is stored in the structure of the synaptic connectivity.

activation may self-sustain by reverberation of activity through the strong connections that link neurons within the Hebbian assembly.

In a seminal theoretical study that paved the way for the continuous attractor concept, Amari<sup>89</sup> showed that stable localized activity patterns can be maintained in networks in which neurons are arranged on a ring, such that the excitatory connections of each neuron decrease progressively with distance on the ring, whereas inhibitory connections increase (Mexican hat connectivity). Since this study, continuous attractors have been used to model various sensory and non-sensory processes, ranging from motor-cortex representations of movement trajectories<sup>90</sup>, orientation selectivity in V1 (REFS 91,92), eye position<sup>93</sup>, directional tuning of head direction cells<sup>94,95</sup> and the position of an animal in space, as represented by the firing of hippocampal place cells<sup>87,96–99</sup>.

The fact that grid cells maintain their activity pattern after removal of light or other sensory stimuli points to a self-sustaining mechanism<sup>8</sup>. Not surprisingly then, soon after the discovery of grid cells, several continuous attractor models were introduced to explain the formation of spatially periodic firing<sup>3,100,101</sup> (FIG. 2). All of these models have two stages. First, cells are arranged on a matrix according to grid phase. Localized activity (a ‘bump’) is formed when the network has Mexican hat connectivity; that is, cells with similar grid phases are connected through excitatory connections, or they receive less inhibition than those with larger phase differences, which

always inhibit each other (FIG. 2a,b). Bumps can be formed at multiple network locations, with competitive interactions leading to the formation of a hexagonal bump pattern on the network array<sup>100,101</sup>, or the bump can be generated at a single location, with periodic firing emerging when the activity bump returns to the same location in a toroidal matrix<sup>3,102</sup>. In either case, once local activity is generated, the bump is moved by path integration in response to asymmetrical speed and direction inputs to the grid cells, mirroring a mechanism that was originally proposed for head direction cells<sup>95</sup>. When the bump follows the animal’s movement, activity is expressed as a grid pattern in each individual cell.

Continuous attractor models with Mexican hat connectivity were able to produce grid patterns, but it was soon found that these models relied on connectivity matrices that were different from those of key circuits of the MEC. The prime challenge is the almost complete lack of excitatory connections between layer II stellate cells, the cell type containing the largest number of grid cells and the most regular grid patterns<sup>9,26,103–105</sup>. Paired recordings have shown that excitatory connections are nearly absent among stellate cells in adult animals and that stellate cells are instead strongly connected through fast-spiking inhibitory interneurons<sup>106–108</sup>. The inhibition between pairs of stellate cells seems to be consistent in magnitude — that is, all-or-none<sup>107</sup>.

In response to the lack of excitatory connections between stellate cells, it was shown that attractor models can function with only inhibitory interconnections<sup>107–109</sup> (FIG. 2c–f). In the presence of external excitatory drive, neural activity in an inhibitory network self-organized into a stable hexagonal pattern. Competitive inhibitory interactions drove activity to maximally spaced positions. As in the earlier excitatory models, a path-integration mechanism could be used to move the activity bumps across the neuronal lattice in accordance with the animal’s movement. The emergence of grid patterns in purely inhibitory networks has also been shown in a previous study of Mexican hat connectivity in which inhibition decreased progressively as grid phases became more similar<sup>101</sup>. The dependence on tonic external excitatory drive predicted by these models has been verified in a study in which hippocampal projections to the MEC were silenced by infusion of a GABAergic agonist in the hippocampus<sup>109</sup>. Infusions led to substantial drops in the firing rates of grid cells, accompanied by a progressive loss of grid structure and the appearance of directional tuning, as expected when residual external inputs take over as determinants of grid cell firing. Similar disruptions of grid cell firing have been observed under other conditions that reduce excitatory input to grid cells<sup>110,111</sup>.

The relationship between external excitatory input and grid structure verifies one prediction of the inhibitory models but far from proves any of them. These models demonstrate that inhibitory connections, such as those that connect layer II stellate cells, are sufficient for activity to self-organize into a hexagonal pattern. However, whether this actually is the mechanism of grid cell formation remains to be determined. Per today, in

#### Continuous attractor

An attractor network in which the collection of attracting points form not a discrete set but a continuum (a ring or a sheet).

#### Mexican hat connectivity

The connectivity of networks in which neurons are arranged on a ring or sheet such that the excitatory connections of each neuron decrease progressively with distance, whereas inhibitory connections increase in strength.

#### Stellate cells

Morphologically defined as cells with a round soma and dendrites radiating from it in all directions. In the medial entorhinal cortex, stellate cells are the main origin of the projection to the dentate gyrus and CA3.

### Box 3 | The problem of drift in attractor networks

One major challenge faced by all continuous attractor models comes from the requirement of translational invariance: this means that if a pair of neurons with distance  $d$  are connected with a connection of strength  $W$ , the connection between every other pair of neurons with distance  $d$  should have the same strength  $W$ . In such a network, if a bump of activity centred at one point is stable, every translation of it on the network is also stable. The bump can be moved smoothly across the network with a little push by an external input and will stay still when the input is gone.

Real networks do not share this idealized connectivity pattern. The existence of inhomogeneity in the connectivity, or of other sources of noise, breaks the translational invariance, leading to a fragmentation of the continuum of attractors<sup>95,96,201,202</sup>. Not all positions will then be stable positions of the bump, but only a small number of them. As a result, a bump of activity, initialized at a given position, instead of staying there until an external input moves it, will spontaneously drift away towards one of the few stable positions. This fragmentation of the continuum would interfere with path integration.

In the case of working memory, when the position of a bump of activity represents the position of an object in the external environment, different solutions to the drift problem have been proposed, including short-time homeostatic synaptic plasticity<sup>201</sup>, gain modulation<sup>202</sup> and synaptic facilitation<sup>203</sup>. In the case of synaptic facilitation, synaptic weights are temporarily increased between neurons in the bump, thereby increasing the connectivity between these neurons and their activity, and enhancing the resistance of the bump to movement by noise. Irrespective of implementation, such changes should be short-lasting; otherwise, the bump would remain in place when a move is needed, for example, to represent a new position.

Although short-term plasticity might alleviate drift in working memory models, such mechanisms have not been tested for networks in which the bump should continuously track an external input, such as attractor networks of grid cells or place cells. Furthermore, the suggested mechanisms have a potential drawback: changes in synaptic weight or single-neuron gain may negatively interfere with the retrieval of information that is already stored in the distribution of synaptic efficacies<sup>202</sup>. A complete answer to the problem of drift caused by inhomogeneity in attractor models of grid cells is lacking.

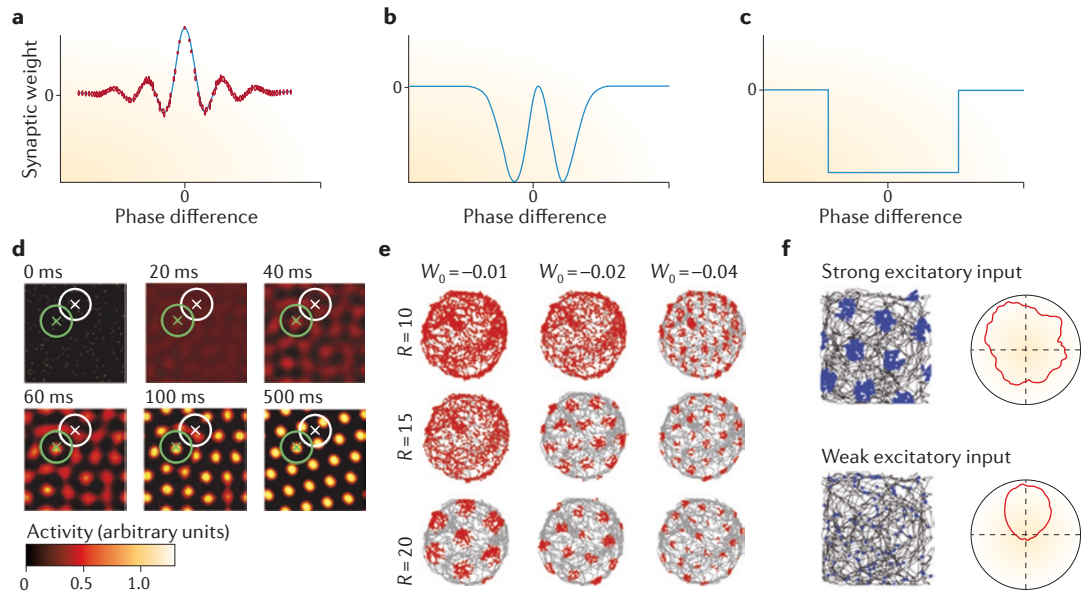


**Figure 2 | Excitatory and inhibitory attractor models for grid cells.** **a–c** | A variety of connectivity patterns have been used in attractor models of grid cells to generate hexagonal firing patterns. These include the Mexican hat connectivity used by Fuhs and Touretzky<sup>100</sup> (part **a**), the Mexican hat-like connectivity of Burak and Fiete<sup>101</sup> (part **b**) and the step-like inhibitory connectivity used by Couey *et al.*<sup>107</sup> (part **c**). The connectivity patterns differ in the complexity of the phase dependence of the synaptic weights. In models with Mexican hat connectivity, cells have progressively decreasing excitatory connections combined with increasing inhibitory connections, whereas the Mexican hat-like connectivity model and the step-like connectivity model use purely inhibitory connections, although the inhibitory fields have different shapes. All three connectivity patterns produce a hexagonal grid pattern. **d** | The step-like connectivity model leads to the spontaneous formation of a hexagonal grid pattern. Successive sheets illustrate the network at different developmental stages (0 to 500 ms), with individual pixels corresponding to individual neurons and neurons arranged according to grid phase in each sheet. Activity of neurons is colour-coded, as indicated by the scale bar. Connection radii  $R$  of two example neurons are shown as white and green circles (diameter  $2R$ ). **e** | Single-neuron activity (red dots) in a circular arena from the simulation in part **d**.  $W_0$  is the strength of the inhibitory connectivity. It can be seen that  $W_0$  and  $R$  control the size of the grid fields and their spacing. **f** | External excitatory drive is necessary for grid formation. Spike distribution plots (on the left, as in part **e**) and directional tuning curves (firing rate as a function of direction, on the right) with strong excitatory output and weak excitatory input. When the external input drops below a critical amount, the activity on the neuronal sheet is vulnerable to distortions, and the hexagonal structure is not detectable in time-averaged plots. At the same time, head direction input becomes the dominant source of input and cells become directional. Parts **d** and **e** from REF. 107, Nature Publishing Group. Part **f** from REF. 109, Nature Publishing Group.

the absence of further theoretical development and new experimental data, the high demands that attractor models put on network connectivity disallow them to be adopted as straightforward explanations of grid cells (BOX 3).

**Assumptions about recurrent connectivity**

Attractor models of grid cells require neurons to be connected to each other, directly or indirectly, by way of synaptic weights that depend on the phase difference between neurons<sup>3,100,101,107</sup>. Whether developmental processes allow for the complexity of such a wiring scheme is an open question. The salt-and-pepper-like organization of the grid network<sup>8</sup> implies that preferential coupling between phase-matched cells cannot be obtained merely by letting cells connect to their nearest neighbours.

One possibility is that grid cells overcome the lack of topography by connecting, directly or indirectly, to cells with similar grid phases irrespective of distance. There is some precedence for connective specificity

between distributed but functionally similar neurons in V1 of the visual cortex, where cells that code for specific orientations are frequently connected, whereas cells with different orientation preferences are connected more rarely<sup>112–115</sup>. If cells with similar grid properties wire together similarly in the MEC, how could they find each other? A study by Li *et al.*<sup>59</sup> used *in utero* electroporation to label cells from one developmental clone in V1. At adult age, sister neurons from this clone were not only more strongly connected but also more similarly tuned for orientation and direction than randomly selected neighbouring neuron pairs. These neurons were initially connected by gap junctions, which later gave way to chemical synapses. We do not know whether connective topography between phase-matched cells within modules in the MEC has a similar developmental origin.

The development of lateral connectivity becomes simpler if the connectivity problem is reduced from two dimensions to one. This has been suggested in a two-step model by Grossberg and colleagues<sup>116,117</sup>. In the

**Box 4 | Oscillatory interference models of grid cells**

Several models have been developed to explain the formation of grid patterns in medial entorhinal cortex (MEC) cells. Historically, the majority of the models have fallen into one of two classes — attractor network models and oscillatory interference (OI) models. Network models are subject to extensive ongoing research and have been described in the main text. In this box, we briefly review the key features of the OI models.

The core idea of OI models is that spatially periodic firing arises as a consequence of interference between a relatively constant global theta oscillation and a velocity-controlled cell-specific theta oscillation<sup>80–82</sup>. The frequency of the cell-specific theta oscillation is determined by the projection of the animal's velocity in a certain running direction. Interference between the global oscillator and the velocity-controlled oscillator gives rise to spatial bands of activity along the preferred orientation of the latter. Different velocity-controlled oscillators have preferred directions that are separated by 60 degrees, such that their combined input, together with the global theta oscillation, results in a hexagonal firing pattern in a target cell that receives all of these inputs. In the first generation of models, a triplet of oscillators was put into the same neuron. Later models recognized that multiple oscillators in the same neuron would phase-lock at behavioural timescales<sup>204</sup>, so the velocity-controlled oscillators were put into separate groups of afferent neurons<sup>205,206</sup>.

OI models have successfully explained some properties of temporal organization in grid cells, such as theta phase precession<sup>105,207</sup>, an aspect that has not been addressed in attractor models, except in one dimension<sup>208</sup>. However, OI models have faced serious challenges as an explanation of the spatial periodicity of the grid cells. Experimental testing has failed to verify two of the key assumptions of the OI models. First, although grid formation in these models requires theta oscillations, grid cells have been observed in the absence of theta activity in fruit bats<sup>17</sup> as well as macaque monkeys<sup>21</sup>. In these species, theta oscillations are intermittent and the formation of grid patterns occurred regardless of whether theta activity was present or not. Theta resonance was not present in stellate cells from bats<sup>209</sup>. A similar dissociation was noted after knockout of the genes encoding HCN1 (hyperpolarization-activated cyclic nucleotide-gated channel 1) channels, which almost completely abolishes theta resonance<sup>210</sup> but leaves grid patterns intact despite some expansion in the scale of the grid<sup>211</sup>. A second challenge is the failure to verify the proposed coincidence between grid fields and theta interference waves in the membrane potential of grid cells. Whole-cell recordings from head-fixed mice running in virtual environments showed minimal links between grid periodicity and amplitude of the theta oscillation<sup>104,105</sup>, contrary to the predictions from the OI models. OI models were only able to account for the data if attractor dynamics were introduced in addition<sup>105,212</sup>. Taken together, these experimental observations provide strong evidence against the simplest forms of theta-based OI models for grid formation, although interference can in principle happen at lower or higher frequencies<sup>213</sup> if MEC cells resonate at those frequencies.

From a theoretical perspective, the OI model has from the beginning had the weakness that the 60-degree periodicity must be manually inserted into the model; that is, the emergence of 60-degree periodicity was explained by a similar regularity in the input to the cells. In the OI models, cells receive input from one-dimensional oscillators that are separated by 60 degrees. It is this separation that has remained unexplained. In 2012, Mhatre *et al.*<sup>116</sup> proposed a model in which, instead of using interference of theta and a velocity-dependent oscillation, they used ring attractors to generate stripe-like responses. They showed, through computer simulations, that when the stripes do not share the same phase or orientation, grid cells can be generated by choosing stripes that are separated from each other by 60 degrees through a self-organizing process. As the self-organization map does not depend on how the stripes are generated, at least not when they are perfect stripes, the mechanism proposed by Mhatre *et al.* can be used in OI models to solve the 60-degree separation. However, the two models (Mhatre *et al.* and OI) will most likely respond differently to noise during self-organization. In particular, the Mhatre *et al.* model may take advantage of the synaptic and gain modulation mechanism that can be used for removing drift (BOX 2). A related explanation has been provided more recently by Hasselmo and Brandon<sup>214</sup> who proposed a model in which the grid pattern emerges through attractor dynamics based on an effective connectivity similar to that of Fuhs and Touretzky<sup>100</sup> but mediated by oscillatory cells with head directional selectivity and reciprocal connections to grid cells.

first step, a set of ring attractors are formed upstream of the grid cells. Each ring attractor encodes a selected direction of movement in external space, and a bump on the ring attractor will path integrate the movement of the animal along that direction based on velocity input. The cells in each ring thus respond as bands that cover the space in a direction that is orthogonal to the preferred direction of the ring attractor. In the second step, the ring attractors contact grid cells with projections that are subject to competitive learning. The competitive learning is shown to select ring attractors with 60-degree separation of preferred orientations, leading to hexagonal grid firing.

One-dimensional attractor networks are appealing because they put considerably less demand on the specificity of wiring between grid cells. Coupling with phase-matched cells would only be required in one direction. However, the Grossberg model does not explain how the connectivity of the ring attractors is formed, and analytical proof of the self-organizing mechanism is yet to be obtained. Also, the location of the proposed ring attractors remains elusive. Some grid cells in the deeper MEC layers show somewhat different degrees of periodic firing along the three grid axes<sup>9,26</sup>, raising the possibility that such cells respond to cells with band-like activity<sup>26</sup>, but 'band cells' have not been observed in or near the MEC to date.

Several studies have recently tried to determine whether grid cells with similar grid phases are preferentially coupled, as required by the two-dimensional attractor models. In a recent study, channelrhodopsin 2 was selectively expressed in parvalbumin-expressing MEC interneurons<sup>118</sup>. Cross-correlation analyses showed that rate maps of pairs of grid cells that projected to the same parvalbumin-expressing interneuron were no more similar than randomly chosen cells. At first glance, this finding seems to be at odds with attractor models based on inhibitory coupling of grid cells with similar grid phase. However, cross-correlated activity may reflect common but time-shifted inputs rather than synaptic connections<sup>119</sup>. The proportion of such false negatives in the data is not known. Furthermore, inhibitory postsynaptic potentials are often elicited only after strong and coincident stimulation of multiple inputs to cells<sup>107</sup>, suggesting that although the interneurons may receive input from grid cells with a broad spectrum of grid phases, their output may depend on restricted subsets.

An alternative way to determine functional connections between grid cells is to analyse the entire pattern of co-activity in large samples of simultaneously recorded neurons. Mathis *et al.*<sup>120</sup> analysed data from grid cells on a one-dimensional track showing that noise correlation among these cells decays as the phase difference increases. In another study<sup>121</sup>, a kinetic Ising model<sup>122</sup> was used to infer effective connections in a population of 27 grid cells recorded simultaneously in an open field. Inferred connections between pairs of grid cells decayed with increasing phase difference, starting as positive for neurons with nearly identical phases and turning to negative at larger phase differences. In a third

study, noise correlations between pairs of simultaneously recorded neurons were used as a proxy for the functional connections between pairs of grid cells<sup>123</sup>. Again, noise correlations were found to decay steeply with phase differences, as predicted if grid cells with similar phases were preferentially coupled.

Thus, there is some evidence in favour of specific functional connectivity between cells with similar grid phases, but the implementation of the attractor mechanism, if it exists, is not well understood. We do not know whether the effective connections are excitatory or inhibitory, how connections vary between and within layers and modules or how they change through learning and development.

### Grid cells in feedforward networks

The recurrent inhibitory network of MEC layer II is not functional until rats are almost 4 weeks old<sup>124</sup>. Rudimentary grid cells can be observed before this age, although the grid fields are noisier, less periodic and less stable<sup>124,125</sup>. This split raises the question of whether grid cells can be formed in the absence of recurrent networks. Kropff and Treves<sup>126</sup> have developed a model in which entorhinal neurons receive spatial information through plastic feedforward connections. These entorhinal neurons are subject to neuronal fatigue or adaptation. In combination with fixed sparsity in network activity, which is presumably enforced by inhibitory processes, adaptation leads to changes in the strength of the feedforward connections, such that the firing pattern of individual neurons becomes hexagonal. Initially, feedforward weights are random and neurons fire at random places depending on fluctuations in the inputs they receive. After a brief period of above-average activity, neurons tend to be suppressed as a result of adaptation. When a neuron is firing, its active feedforward connections are enhanced through plasticity, whereas the inactive ones are suppressed. When the firing is suppressed, no synaptic modification occurs. Slowly, upon extensive averaging over many trajectories, the synaptic modification among active neurons causes, in each cell, a regular pattern of firing fields embedded in a matrix of non-firing regions, as the rat navigates in space. Unlike the attractor models, the adaptation model does not require preferential connections between grid cells with similar phases and activity is not translated across the network in a speed- and direction-dependent manner. Thus, there is no path integration in this model, although some of the spatial information expressed in the feedforward inputs may be based on path integration, which is computed elsewhere.

In the simplest version of this adaptation model, the orientation of the emerging grid cells is random. This contrasts with the non-uniform distribution of grid orientation in experimental data<sup>8,24,127</sup>. The problem could be alleviated by including excitatory recurrent collaterals to align the grid cells<sup>126,128</sup>. However, the formation of collaterals would be a time-consuming process that is hard to reconcile with the rapid stabilization of grid cells in novel environments<sup>8</sup>. A solution might be that recurrent collaterals form during development without a need for learning through adaptation in every new environment.

Adaptation and attractor mechanisms are not mutually exclusive possibilities. It is conceivable that grid cells form through a hybrid mechanism by which spatially periodic firing emerges early in development based on adaptation and feedforward plasticity, and that recurrent connections develop subsequently by activity-dependent mechanisms. These recurrent connections may then enable translation of activity in accordance with the animal's movements in external space in a continuous attractor network. An analogy to this sequence has recently been observed in the visual cortex, where selectivity for visual stimuli has been shown to appear in a feedforward network around the age of eye opening, before the development of connections between cells with similar response signals<sup>54</sup>. Precise local connectivity may not be crucial for feature selectivity in individual cells, at least in a rudimentary form, but it may be necessary for the network to acquire attractor and path integration properties.

An important feature of the adaptation model is that it relates the geometry of the environment to the spatial firing pattern of the grid cells. For animals raised in conventional two-dimensional environments, the model predicts hexagonal grids. However, if the animal is raised in a sphere, the model predicts the appearance of regular patterns that range from one activity peak to pentagonal patterns, depending on the radius of the sphere and the parameters of the adaptation<sup>129</sup>. The model also makes predictions about the form of the spatial selectivity in three dimensions<sup>130</sup>. This is particularly relevant for animals that navigate in three-dimensional space, such as bats. As all existing models predict hexagonal patterns on flat surfaces, experiments with animal raised in different geometries<sup>131</sup> will be important for distinguishing between models.

### Uniqueness of the entorhinal grid network

If grid patterns emerge from interactions between large numbers of neurons, grid cells might also exist beyond the MEC in circuits with similar network architectures. However, in tetrode recordings, grid cells have so far only been observed in the MEC and the adjacent pre- and parasubiculum<sup>7,103</sup>. A recent study in human patients with epilepsy reported grid-like activity in what was referred to as the cingulum<sup>23</sup>, but in the absence of images of electrode location in this report and assuming the most commonly used implantation trajectory in such patients, it is likely that the spikes originate from the nearby pre- or parasubiculum, which in rodents contains a large number of grid cells<sup>103</sup>. As of today, there is no published evidence for grid-like activity in circuits outside a continuous parahippocampal region that consists of the MEC and pre- and parasubiculum.

But would grid cells be found if we searched specifically in regions that share the recurrent connection patterns of the MEC? Recurrent excitatory connectivity is part of the normal architecture of the neocortex, within and between layers<sup>132</sup>. The connectivity can be extensive, such as between spiny stellate cells in layer IV of the barrel cortex, where the estimate is 24% as measured by *in vitro* multipatch recordings<sup>133</sup>, and between pyramidal

#### Recurrent networks

Neural networks in which each neuronal element provides an input onto many of the other neurons in the network.

#### Adaptation

Adaptation refers to the decrease in firing frequency that neurons exhibit following a period of repeated discharge.

cells of the visual cortex, where the connectivity may be even higher<sup>134,135</sup>. Similarly dense connectivity has been observed in several allocortical and allocortical–neocortical transition areas, such as the olfactory cortex<sup>136</sup>, the CA3 of the hippocampus<sup>137–139</sup>, the subiculum<sup>140</sup> and layers III–VI of the MEC<sup>106</sup>. By contrast, there are very few networks with exclusive inhibitory connectivity that is similar to that of MEC layer II. Such networks may exist in the pre- and parasubiculum, where whole-cell recordings following locally applied stimulation suggest that excitatory connections in layers II and III are sparse<sup>141</sup>. These data need to be confirmed by direct recordings from cell pairs, but the possibility of exclusive inhibitory connectivity in just those areas that exhibit grid patterns is intriguing.

However, there are two regions outside the allocortical parahippocampal cortex, where inhibitory interconnections are as predominant as in layer II of the MEC. One is the olfactory bulb, where a major class of excitatory neurons — mitral cells — is almost exclusively connected through inhibitory granule cells<sup>142</sup>. The second area is the dentate gyrus. Mossy fibres from dentate granule cells collateralize extensively in the hilus, where they preferentially target interneurons that project back to the granule cells<sup>143,144</sup>. No direct excitatory connections have been reported between granule cells<sup>143,144</sup>. Thus, the olfactory bulb and the dentate gyrus contain several key elements of MEC architecture; however, grid cells have not been reported in these areas. The olfactory bulb is clearly outside the spatial system of the brain. Dentate granule cells have multiple discrete firing fields<sup>145</sup> but they lack spatial periodicity<sup>146</sup>. The lack of grid pattern in granule cells may reflect several differences between the MEC and dentate gyrus circuitry — for example, the possible absence of direct inputs to the dentate gyrus from speed and head direction cells, or the strongly hyperpolarized membrane potential of the granule cells<sup>147</sup>. In the MEC, the hexagonal structure of grid cell activity is lost after removal of excitatory input and, by implication, hyperpolarization of the cell membrane<sup>109</sup>.

If layer II of the MEC has unique properties, which cell types in this layer produce grid cells? Layer II grid cells could be either stellate cells or pyramidal cells. Because two-thirds of the excitatory layer II cells are stellate cells<sup>148</sup> and at least one-half have grid properties<sup>9,103</sup>, a considerable fraction of the grid cells may be stellate cells. This is consistent with studies in which grid cells were recorded intracellularly from head-fixed mice in virtual environments<sup>104,105</sup>. In these studies, the majority of layer II grid cells had stellate-specific morphological and electrophysiological properties. The suggestion that many grid cells are stellate cells is consistent with the fact that stellate cells are the main origin of the layer II projections to dentate gyrus and CA3 (REFS 149, 150), and the fact that grid cells are abundant among hippocampus-projecting MEC neurons<sup>146,151</sup>. Nonetheless, these observations do not rule out that some grid cells are pyramidal cells. Grid cells are also present in deeper MEC layers<sup>9</sup>, which have no stellate cells<sup>152,153</sup>. The pyramidal cells may use a mechanism that is different from the inhibitory

mechanism in layer II and more like the Mexican hat excitatory–inhibitory architecture originally proposed for grid cells<sup>3,100,101</sup>, or alternatively the grid pattern could merely be propagated through connections from stellate cells. Intracellular recordings and staining of larger numbers of cells in behaving animals will have to be carried out before conclusive statements can be made about the cellular identity of grid cells. It is important to solve this question, considering the central role that the stellate cell network has in some attractor models for grid cells.

### Grid cells and place field formation

The entorhinal representation of space is complemented by a map of place cells in the hippocampus<sup>2,5,6</sup>. A striking difference between grid cells and place cells is that place cells, unlike grid cells, often remap completely between environments and even between experiences in the same environment<sup>10,11,154,155</sup>. Whereas ensembles of grid cells exhibit spatially coherent firing patterns across tasks<sup>12</sup>, the active subset of place fields may be almost completely replaced, and among cells that are still active, the combination of firing locations is usually different. Thus, the entorhinal–hippocampal circuit has two maps of space. One map expresses the metrics of the environment independently of its specific configuration of landmarks (grid cells), and the other map consists of semi-orthogonal representations that are unique to individual environments (place cells); that is, a map of space in general and a large number of maps for particular spaces.

Since the discovery of the grid cells, it has been asked whether place cells originate by transformation of input from grid cells one synapse upstream, in layers II and III of the MEC. In the same way that orientation-selective cells were suggested to originate by linear summation from concentric circular fields in the visual cortex<sup>156</sup>, place cells have been proposed to emerge by linear summation of output from grid cells with overlapping grid phase but different grid scale<sup>3,100,157,158</sup>. At the same time, however, other models suggested that place fields can be generated from any weak spatial input — periodic or non-periodic — so long as the local hippocampal circuit contains mechanisms for local signal amplification through recurrent networks or Hebbian plasticity<sup>159–162</sup>. The relationship between grid cells and place cells was further complicated by experimental data suggesting that not only grid cells but also other functional cell types project from the MEC to the hippocampus<sup>151</sup>. The input from entorhinal border cells is of particular interest because early computational models pointed to such cells as a potential origin of place-selective activity<sup>163,164</sup>. These models suggested that place cells receive input from hypothesized ‘boundary vector cells’ in the cortex outside the hippocampus — cells whose firing rates reflect distance and direction to specific boundaries of the local environment. Border cells in the MEC constitute a specific subset of such cells, but they fire only at the borders. Responses with peaks at increasing distance from the borders have been observed in the subiculum<sup>75,76</sup> but not among hippocampus-projecting cells in the MEC<sup>73,74,151</sup>. The larger number of hippocampal place

fields near corners and walls of recording environments compared with central areas<sup>165–167</sup> is consistent with a contribution by entorhinal border cells in place field formation. Considering that border cells have adult-like characteristics from the first day of outbound exploration in rat pups<sup>168</sup>, inputs from such cells may explain the conundrum that place cells mature earlier than grid cells<sup>124,125</sup>, contrary to the predictions of the linear summation model for grid-to-place cell transformation. The findings raise the possibility that border cells play a part in driving place cells in young animals and that grid inputs have an increasingly important role as the animals get older, possibly with a stronger contribution to the metrics of the place representation. Whether this development is accompanied by an increasing ability of place cells to map environments based on path integration remains to be determined.

Although the hippocampus seems to receive inputs from various entorhinal cell types, it is not yet clear whether the input to an individual hippocampal place cell is functionally diverse or dominated by input from one particular functional class of neurons — for example, grid cells. If the input is mixed, an obvious question is how inputs are selected and transformed into stable and spatially confined firing fields. Some clues can be obtained from studies of synaptic input to orientation-selective neurons in area V1 of the visual cortex. In one study, synaptic inputs were mapped in response to drifting gratings by imaging of calcium responses across spines of individual neurons in layer II or III of area V1 (REF. 169). The study showed heterogeneity in orientation preferences across dendritic spines, although some cells displayed quite homogeneous dendritic responses. A subsequent study using a more sensitive calcium indicator and a considerably larger cell sample confirmed that synaptic inputs are heterogeneous but also showed that the output of the cell could be predicted from the average tuning of the synaptic inputs<sup>170</sup>. Similar heterogeneity may be present in the entorhinal inputs to individual place cells. If so, the properties of the place field may be determined not only by the relative numbers of different functional inputs but also by variations in synaptic strength, dendritic mechanisms within the target cell and local circuit mechanisms.

The availability of a broad spectrum of entorhinal inputs has potential advantages for the information encoded in a hippocampal place cell. Connectivity with multiple cell types allows for dynamics in the functional coupling of entorhinal and hippocampal cell assemblies. Gamma oscillations provide a mechanism for dynamic coupling of selected cell assemblies<sup>171,172</sup>. Place cells in CA1 use fast gamma oscillations to couple to spatially modulated cell assemblies in the MEC<sup>173</sup>, whereas low-frequency beta–gamma oscillations enable coupling with odour-coding neurons in the lateral part of the entorhinal cortex<sup>174</sup>. Because beta and gamma epochs are both short-lasting and regionally specific<sup>173,174</sup>, place cells may interact dynamically with a range of entorhinal cell assemblies, which each carry a distinct type of information. The efficiency of individual functional inputs depends on behaviour, such as running speed<sup>175</sup>,

and evolves in parallel with behavioural learning<sup>174</sup>, suggesting that the balance between inputs to a place cell is experience-dependent.

Finally, connections between spatial cells in the MEC and hippocampus are bidirectional. Although grid cells or border cells may be essential for the formation of place cells, place cells are also likely to influence spatial maps in the MEC through direct or indirect connections (BOX 2). When the hippocampus is inactivated, the hexagonal firing pattern of the grid cells is lost and the cells instead become responsive to other influences such as head direction signals<sup>109</sup>. The elimination of grid structure strongly correlates with the induced drop in firing rates of the grid cells and is consistent with the need for external excitatory input proposed by inhibitory network models of grid cells<sup>101,107,108</sup>. The dependence on external excitation, from the hippocampus or elsewhere, does not rule out a role for hippocampal backprojections in other functions of grid cells, such as in updating position coordinates based on environment-specific maps stored in the hippocampus.

### Evolution of grid cells and a wider perspective

Grid cells are not unique to rodents. A recent study reported grid cells in Egyptian fruit bats<sup>17</sup>. Bats belong to the order Chiroptera, which branched off at an early stage of mammalian evolution, before, for example, the separation of rodents and primates<sup>176</sup>. The presence of grid cells in different orders suggests that grid cells appeared early in evolution and so may be present across a wide span of mammalian species. It is even possible that grid cells exist in reptiles, such as lizards, or in bony fish, which have brain circuits that are similar to those of the mammalian hippocampus and which navigate space in ways that are not too different from rodents and bats, respectively<sup>177</sup>. This possibility is reinforced by the fact that navigation in turtles and goldfish depends on homologues of the mammalian hippocampus<sup>178,179</sup>. The fact that all spatially tuned cells described so far are found in phylogenetically old cortical areas is consistent with the idea of a common set of circuit mechanisms for space in widely separated species.

Cells with grid-like properties have recently been reported in primates. In these studies, the subjects did not move around as in the rodent and bat studies. In the first study<sup>21</sup>, monkeys viewed a sequence of images in quick succession. Grid patterns were reported to emerge when spikes were plotted onto a map of the monkey's eye positions, independently of the content of the visual images, suggesting that the grid cells are a part of a system that uses eye movement to determine firing and that firing location is determined by an ocular path integration mechanism. In the second study, grid cells were reported when human subjects with drug-resistant epilepsy navigated between predetermined locations in a virtual environment<sup>23</sup>. In both experiments, grid patterns were substantially noisier than during locomotion in rodents but the periodicity was stronger than expected by chance. The increased noise may reflect that monkeys occasionally reset the ocular path integrator between images and that human subjects alternated

between virtual and real-world reference frames. Rodent studies have shown that changes in reference frames can occur frequently in grid cells during testing in environments with a complex structure<sup>32</sup>. Such alternations would by necessity reduce periodicity in time-averaged rate maps. The less accurate electrode placement in the human studies and the averaging of activity in multiple layers and subfields are also likely to add noise to the grid pattern. The existence of visually driven grid cells

is reminiscent of spatial view cells in hippocampal and parahippocampal regions of monkeys<sup>19,20</sup>. View cells are cells that respond to the position at which the monkey is looking rather than the animal's position in space. Visually driven grid cells may provide an important input to view cells.

The existence of grid patterns during visual scanning and virtual locomotion suggests that evolution has expanded the range of velocity inputs that may drive the path integrator that is thought to update the grid map as the animal moves through space. It will be interesting to see whether the same cells that respond to visual movement in monkeys also respond to locomotion, or whether there is a separate system of grid cells that is responsive to locomotion. Regardless of the answer, the primate data raise the possibility that grid cells can be used as an internal metric for a range of spatial operations.

### Box 5 | Exploiting new technologies

Looking forward, one of the most exciting avenues of research on grid cells is the application of molecular genetic techniques. The excitement is about the opportunities that these tools offer to learn about how complex internal representations of external space are generated, and how they impinge upon downstream neurons. There are various transgenic driver lines that can be used to express transgenes in different populations of both excitatory and inhibitory neurons in the medial entorhinal cortex (MEC). The modularity of these driver lines is a key advantage: depending on the 'payload' transgene (which can be delivered either by another transgenic line or a complemented virus), one can carry out distinct operations on the same genetically identified sets of cells. The precise cellular identity of grid cells is not yet clear. They may not have precise molecular determinants, so it may be impossible to make a 'grid cell-specific' driver line. Nevertheless, pairing recordings from the MEC of behaving mice with manipulations of specific cell types can be extremely fruitful. Moreover, there already exists a driver line that is almost exclusively expressed in layer II of the MEC<sup>215</sup>, where grid cells are most abundant. First, the identity of grid cells can be determined by optogenetically stimulating different molecularly identified classes of neurons during recordings to see which driver lines are enriched in neurons with certain receptive fields (for example, grid cells). The activity of defined sets of neurons can then be manipulated either optogenetically<sup>216</sup> or pharmacogenetically<sup>217</sup> concomitant with unit recordings, and the effects on the receptive fields of these neurons and other neurons, even far downstream, can be monitored.

Advances in imaging and fluorescent indicator transgenes<sup>170,218–223</sup> now confer the ability to observe the firing of large numbers of genetically defined neurons at once. This enables a shift from the analysis of single or small ensembles of neurons to the analysis of substantial parts of entire neural networks of a brain region. Importantly, this has recently been combined with virtual reality approaches<sup>33,34,224</sup>, which enable manipulations of space that are hard or impossible to achieve in the real world (for example, 'teleportation' of an animal to a different place in the virtual environment<sup>155</sup>). The ability to record the activity of hundreds of neurons, together with their cellular identity and location in the cortical sheet combined with a virtual environment that can be manipulated at will, provides an extremely rich repertoire of experimental possibilities that was unthinkable only few years ago.

The application of these methods could provide empirical tests of models of grid and place cell formation. For example, the role of inhibitory neurons in grid firing postulated here and elsewhere can be tested by using the various interneuron-specific Cre lines<sup>225</sup> that are available to pharmacogenetically stimulate and/or inhibit particular classes of inhibitory neurons during grid cell recordings. Similarly, the role of oscillations in grid cell firing could be investigated by using local field potential recordings as a trigger<sup>226</sup> to drive optogenetic manipulation relative to the phase of local oscillations. The role of plasticity in the development of the receptive fields of MEC layer II neurons could be investigated by knocking out the genes encoding NMDA receptors in a subpopulation of them, and activity-dependence could be assayed by pharmacogenetically depolarizing and/or hyperpolarizing them during development. The identity of the manipulated neurons can subsequently be determined by optogenetic stimulation with bicistronic transgene cassettes. Finally, the anatomical connectivity of specific genetically identified neurons can be determined using appropriate driver lines to target viral-tracing tools such as the G-deleted recombinant rabies system<sup>227,228</sup>, which can deliver transgene payloads specifically to monosynaptic inputs. One can then determine the functional nature of inputs to MEC neurons and establish which receptive fields must combine to make a grid-like receptive field. All in all, these tools make something that just years ago was simply unimaginable — the mechanistic dissection of so complex and cognitive a receptive field as that of the grid cell — entirely plausible.

### Conclusion

The outside world is represented at multiple levels of the cortical hierarchy, from early stages of the primary sensory cortices to the highest levels of the association cortices. At the peak of abstraction is the representation of external space in the MEC and the hippocampus, which has been reviewed in this article. A key cell type of the MEC representation is the grid cell. The hexagonal firing pattern of this cell type provides one of the most striking examples of a neural recreation of the outside world that cannot be traced back in any straightforward way to particular activation patterns of sets of sensory receptors. Unlike for most cell types in the primary sensory cortices, the most salient features of grid-like receptive fields are likely to arise within the entorhinal circuit itself. Grid cells thus provide us with a unique window into high-level computation in the cortex.

The internal origin of the grid pattern is one of the features that makes it such a powerful system for the study of cortical computation. In one sense, the inability to trace signals back to the periphery is a disadvantage, as one cannot manipulate the animal's sensory environment and easily interpret the resulting changes in receptive fields. In another sense, however, the relative lack of sensory determinism enables one to study how the cortex creates complex receptive fields purely out of local neural interactions. Of course, the same is probably true for other higher-level association cortices, but although the relevant input parameters to the spatial receptive fields of entorhinal–hippocampal neurons may indeed be obscure, the representation of environmental space is somewhat unique in that it provides an easily interpretable metric of the output of the computation.

With the recent development of a wide repertoire of circuit tools (BOX 5), we are now in a position to address in detail the mechanisms by which multiple functionally discrete cell types interact to form a representation that is used for a range of functions, spanning from navigation and action guidance to storage of high-capacity declarative memory. The detachment from sensory inputs and the quantitative relationships revealed in

the organization of the grid cell circuit provide potential means for deciphering mechanisms of pattern formation and pattern transformation that may apply widely across the cortex, including the lower levels of the representational hierarchy, where the components of the computational machinery are often more

accessible for experimental testing. By opening doors to pattern formation processes, grid cells may offer an opportunity to get a better understanding of one of the fundamental tasks of the neocortex — to optimize representation and processing of information about the outside world.

1. Felleman, D. J. & van Essen, D. C. Distributed hierarchical processing in the primate cerebral cortex. *Cereb. Cortex* **1**, 1–47 (1991).
2. O'Keefe, J. & Nadel, L. *The Hippocampus as a Cognitive Map* (Clarendon, 1978). **A seminal book proposing hippocampal place cells as the basis of a 'cognitive map' of the animal's external environment. The cognitive map is suggested to be critical for navigation and to provide a basis for memory more generally.**
3. McNaughton, B. L., Battaglia, F. P., Jensen, O., Moser, E. I. & Moser, M. B. Path integration and the neural basis of the 'cognitive map'. *Nature Rev. Neurosci.* **7**, 663–678 (2006). **Along with Fuhs and Touretzky (reference 100), this paper is the first to propose that Turing pattern formation and continuous attractors informed by phase-dependent neural connectivity are the underlying mechanism of grid cells.**
4. Moser, E. I., Kropff, E. & Moser, M.-B. Place cells, grid cells, and the brain's spatial representation system. *Annu. Rev. Neurosci.* **31**, 69–89 (2008).
5. O'Keefe, J. & Dostrovsky, J. The hippocampus as a spatial map. Preliminary evidence from unit activity in the freely-moving rat. *Brain Res.* **34**, 171–175 (1971). **The paper that started it all: the first description (albeit mainly qualitative) of hippocampal place cells.**
6. O'Keefe, J. Place units in the hippocampus of the freely moving rat. *Exp. Neurol.* **51**, 78–109 (1976).
7. Fyhn, M., Molden, S., Witter, M. P., Moser, E. I. & Moser, M. B. Spatial representation in the entorhinal cortex. *Science* **305**, 1258–1264 (2004).
8. Hafting, T., Fyhn, M., Molden, S., Moser, M.-B. & Moser, E. I. Microstructure of a spatial map in the entorhinal cortex. *Nature* **436**, 801–806 (2005). **The discovery of the second distinct kind of receptive field representing external space — the grid cells of the MEC. Grid cells are proposed as the basis for a path integration-dependent attractor network-dependent metric representation of the spatial environment.**
9. Sargolini, F. *et al.* Conjunctive representation of position, direction, and velocity in entorhinal cortex. *Science* **312**, 758–762 (2006).
10. Muller, R. U. & Kubie, J. L. The effects of changes in the environment on the spatial firing of hippocampal complex-spike cells. *J. Neurosci.* **7**, 1951–1968 (1987).
11. Colgin, L. L., Moser, E. I. & Moser, M.-B. Understanding memory through hippocampal remapping. *Trends Neurosci.* **31**, 469–477 (2008).
12. Fyhn, M., Hafting, T., Treves, A., Moser, M.-B. & Moser, E. I. Hippocampal remapping and grid realignment in entorhinal cortex. *Nature* **446**, 190–194 (2007).
13. Rotenberg, A., Mayford, M., Hawkins, R. D., Kandel, E. R. & Muller, R. U. Mice expressing activated CaMKII lack low frequency LTP and do not form stable place cells in the CA1 region of the hippocampus. *Cell* **87**, 1351–1361 (1996).
14. McHugh, T. J., Blum, K. I., Tsien, J. Z., Tonegawa, S. & Wilson, M. A. Impaired hippocampal representation of space in CA1-specific NMDAR1 knockout mice. *Cell* **87**, 1339–1349 (1996).
15. Fyhn, M., Hafting, T., Witter, M. P., Moser, E. I. & Moser, M.-B. Grid cells in mice. *Hippocampus* **18**, 1230–1238 (2008).
16. Ulanovsky, N. & Moss, C. F. Hippocampal cellular and network activity in freely moving echolocating bats. *Nature Neurosci.* **10**, 224–233 (2007).
17. Yartsev, M. M., Witter, M. P. & Ulanovsky, N. Grid cells without theta oscillations in the entorhinal cortex of bats. *Nature* **479**, 103–107 (2011).
18. Ono, T., Nakamura, K., Nishijo, H. & Eifuku, S. Monkey hippocampal neurons related to spatial and nonspatial functions. *J. Neurophysiol.* **70**, 1516–1529 (1993).
19. Rolls, E. T. & O'Mara, S. M. View-responsive neurons in the primate hippocampal complex. *Hippocampus* **5**, 409–424 (1995).
20. Rolls, E. T., Robertson, R. G. & Georges-François, P. Spatial view cells in the primate hippocampus. *Eur. J. Neurosci.* **9**, 1789–1794 (1997).
21. Killian, N. J., Jutras, M. J. & Buffalo, E. A. A map of visual space in the primate entorhinal cortex. *Nature* **491**, 761–764 (2012).
22. Ekstrom, A. D. *et al.* Cellular networks underlying human spatial navigation. *Nature* **425**, 184–188 (2003).
23. Jacobs, J. *et al.* Direct recordings of grid-like neuronal activity in human spatial navigation. *Nature Neurosci.* **16**, 1188–1190 (2013).
24. Stensola, H. *et al.* The entorhinal grid map is discretized. *Nature* **492**, 72–78 (2012). **This study shows that grid cells are arranged in discrete, relatively autonomous 'modules' rather than in a smooth topographic representation such as those found in sensory cortices.**
25. Barry, C., Hayman, R., Burgess, N. & Jeffery, K. J. Experience-dependent rescaling of entorhinal grids. *Nature Neurosci.* **10**, 682–684 (2007).
26. Krupic, J., Burgess, N. & O'Keefe, J. Neural representations of location composed of spatially periodic bands. *Science* **337**, 853–857 (2012).
27. Mittelstaedt, M. L. & Mittelstaedt, H. Homing by path integration in a mammal. *Naturwissenschaften* **67**, 566–567 (1980).
28. Müller, M. & Wehner, R. Path integration in desert ants, *Cataglyphis fortis*. *Proc. Natl Acad. Sci. USA* **85**, 5287–5290 (1988).
29. Etienne, A. S. & Jeffery, K. J. Path integration in mammals. *Hippocampus* **14**, 180–192 (2004).
30. Gothard, K. M., Skaggs, W. E. & McNaughton, B. L. Dynamics of mismatch correction in the hippocampal ensemble code for space: interaction between path integration and environmental cues. *J. Neurosci.* **16**, 8027–8040 (1996).
31. McNaughton, B. L. *et al.* Deciphering the hippocampal polyglot: the hippocampus as a path integration system. *J. Exp. Biol.* **199**, 173–185 (1996).
32. Derdikman, D. *et al.* Fragmentation of grid maps in a multimodal environment. *Nature Neurosci.* **12**, 1325–1332 (2009).
33. Chen, G., King, J. A., Burgess, N. & O'Keefe, J. How vision and movement combine in the hippocampal place code. *Proc. Natl Acad. Sci. USA* **110**, 378–383 (2013).
34. Ravassard, P. *et al.* Multisensory control of hippocampal spatiotemporal selectivity. *Science* **340**, 1342–1346 (2013).
35. Kropff Causa, E., Carmichael, J. E., Baldi, R., Moser, M.-B. & Moser, E. I. Modulation of hippocampal and entorhinal theta frequency by running speed and acceleration. *Soc. Neurosci. Abstr.* **39**, 769.09 (2013).
36. Parron, C. & Save, E. Evidence for entorhinal and parietal cortices involvement in path integration in the rat. *Exp. Brain Res.* **159**, 349–359 (2004).
37. Kim, S., Sapiurka, M., Clark, R. E. & Squire, L. R. Contrasting effects on path integration after hippocampal damage in humans and rats. *Proc. Natl Acad. Sci. USA* **110**, 4732–4737 (2013).
38. Shrager, Y., Kirwan, C. B. & Squire, L. R. Neural basis of the cognitive map: path integration does not require hippocampus or entorhinal cortex. *Proc. Natl Acad. Sci. USA* **105**, 12034–12038 (2008).
39. Biegler, R. Possible uses of path integration in animal navigation. *Animal Learn. Behav.* **28**, 257–277 (2000).
40. Brun, V. H. *et al.* Progressive increase in grid scale from dorsal to ventral medial entorhinal cortex. *Hippocampus* **18**, 1200–1212 (2008).
41. Illig, K. R. & Haberly, L. B. Odor-evoked activity is spatially distributed in piriform cortex. *J. Comp. Neurol.* **457**, 361–373 (2003).
42. Stettler, D. D. & Axel, R. Representations of odor in the piriform cortex. *Neuron* **63**, 854–864 (2009).
43. Ohki, K., Chung, S., Ch'ng, Y. H., Kara, P. & Reid, R. C. Functional imaging with cellular resolution reveals precise micro-architecture in visual cortex. *Nature* **433**, 597–603 (2005).
44. Van Hooser, S. D., Heimel, J. A., Chung, S., Nelson, S. B. & Toth, L. J. Orientation selectivity without orientation maps in visual cortex of a highly visual mammal. *J. Neurosci.* **25**, 19–28 (2005).
45. Bonin, V., Histed, M. H., Yurgenson, S. & Reid, R. C. Local diversity and fine-scale organization of receptive fields in mouse visual cortex. *J. Neurosci.* **31**, 18506–18521 (2011).
46. Gray, C. M., Maldonado, P. E., Wilson, M. & McNaughton, B. Tetraodes markedly improve the reliability and yield of multiple single-unit isolation from multi-unit recordings in cat striate cortex. *J. Neurosci. Methods* **65**, 43–54 (1995).
47. Dombeck, D. A., Harvey, C. D., Tian, L., Loofer, L. L. & Tank, D. W. Functional imaging of hippocampal place cells at cellular resolution during virtual navigation. *Nature Neurosci.* **13**, 1433–1440 (2010).
48. Ziv, L. *et al.* Long-term dynamics of CA1 hippocampal place codes. *Nature Neurosci.* **16**, 264–266 (2013).
49. Mathis, A., Herz, A. V. & Stemmler, M. Optimal population codes for space: grid cells outperform place cells. *Neural Comput.* **24**, 2280–2317 (2012).
50. Wei, X.-X., Prentice, J. & Balasubramanian, V. The sense of place: grid cells in the brain and the transcendental number e. [online], <http://arxiv.org/abs/1304.0031> (2013).
51. Ratliff, C. P., Borghuis, B. G., Kao, Y. H., Sterling, P. & Balasubramanian, V. Retina is structured to process an excess of darkness in natural scenes. *Proc. Natl Acad. Sci. USA* **107**, 17368–17373 (2010).
52. Chapman, B., Stryker, M. P. & Bonhoeffer, T. Development of orientation preference maps in ferret primary visual cortex. *J. Neurosci.* **16**, 6443–6453 (1996).
53. Li, Y., Fitzpatrick, D. & White, L. E. The development of direction selectivity in ferret visual cortex requires early visual experience. *Nature Neurosci.* **9**, 676–681 (2006).
54. Ko, H. *et al.* The emergence of functional microcircuits in visual cortex. *Nature* **496**, 96–100 (2013).
55. Meister, M., Wong, R. O., Baylor, D. A. & Shatz, C. J. Synchronous bursts of action potentials in ganglion cells of the developing mammalian retina. *Science* **252**, 939–943 (1991).
56. Katz, L. C. & Shatz, C. J. Synaptic activity and the construction of cortical circuits. *Science* **274**, 1133–1138 (1996).
57. Ackman, J. B., Burbridge, T. J. & Crair, M. C. Retinal waves coordinate patterned activity throughout the developing visual system. *Nature* **490**, 219–225 (2012).
58. Kirkby, L. A., Sack, G. S., Firl, A. & Feller, M. B. A role for correlated spontaneous activity in the assembly of neural circuits. *Neuron* **80**, 1129–1144 (2013).
59. Li, Y. *et al.* Clonally related visual cortical neurons show similar stimulus feature selectivity. *Nature* **486**, 118–121 (2012).
60. Ohtsuki, G. *et al.* Similarity of visual selectivity among clonally related neurons in visual cortex. *Neuron* **75**, 65–72 (2012).
61. Bonhoeffer, T. & Grinvald, A. Orientation columns in cat are organized in pin-wheel like patterns. *Nature* **353**, 429–431 (1991).
62. Maldonado, P. E., Gödecke, I., Gray, C. M. & Bonhoeffer, T. Orientation selectivity in pinwheel centers in cat striate cortex. *Science* **276**, 1551–1555 (1997).
63. Ohki, K. *et al.* Highly ordered arrangement of single neurons in orientation pinwheels. *Nature* **442**, 925–928 (2006).
64. Hubel, D. H. & Wiesel, T. N. Receptive fields and functional architecture of monkey striate cortex. *J. Physiol.* **195**, 215–243 (1968).

65. Hubel, D. H. & Wiesel, T. N. Receptive fields and functional architecture in two nonstriate visual areas (18 and 19) of the cat. *J. Neurophysiol.* **28**, 229–289 (1965).
66. Tootell, R. B., Switkes, E., Silverman, M. S. & Hamilton, S. L. Retinotopic organization. *J. Neurosci.* **8**, 1531–1568 (1988).
67. Ts'o, D. Y., Frostig, R. D., Lieke, E. E. & Grinvald, A. Functional organization of primate visual cortex revealed by high resolution optical imaging. *Science* **249**, 417–420 (1990).
68. Shoham, D., Hübener, M., Schulze, S., Grinvald, A. & Bonhoeffer, T. Spatio-temporal frequency domains and their relation to cytochrome oxidase staining in cat visual cortex. *Nature* **385**, 529–533 (1997).
69. Chen, G., Lu, H. D. & Roe, A. W. A map for horizontal disparity in monkey V2. *Neuron* **58**, 442–450 (2008).
70. Kara, P. & Boyd, J. D. A micro-architecture for binocular disparity and ocular dominance in visual cortex. *Nature* **458**, 627–631 (2009).
71. Ranck, J. B. Jr. in *Electrical Activity of the Archicortex* (eds Buzsáki, G. & Vanderwolf, C. H.) 217–220 (Akademiai Kiado, 1985).
72. Taube, J. S., Muller, R. U. & Ranck, J. B. Jr. Head-direction cells recorded from the postsubiculum in freely moving rats. I. Description and quantitative analysis. *J. Neurosci.* **10**, 420–435 (1990).
73. Savelli, F., Yoganarasimha, D. & Knierim, J. J. Influence of boundary removal on the spatial representations of the medial entorhinal cortex. *Hippocampus* **18**, 1270–1282 (2008).
74. Solstad, T., Boccara, C. N., Kropff, E., Moser, M.-B. & Moser, E. I. Representation of geometric borders in the entorhinal cortex. *Science* **322**, 1865–1868 (2008).
75. Barry, C. *et al.* The boundary vector model of place cell firing and spatial memory. *Rev. Neurosci.* **17**, 71–97 (2006).
76. Lever, C., Burton, S., Jeewajee, A., O'Keefe, J. & Burgess, N. Boundary vector cells in the subiculum of the hippocampal formation. *J. Neurosci.* **29**, 9771–9777 (2009).
77. Hubel, D. H. & Livingstone, M. S. Segregation of form, color, and stereopsis in primate area 18. *J. Neurosci.* **7**, 3378–3415 (1987).
78. Yoon, K. *et al.* Specific evidence of low-dimensional continuous attractor dynamics in grid cells. *Nature Neurosci.* **16**, 1077–1084 (2013).
79. Barry, C., Ginzberg, L. L., O'Keefe, J. & Burgess, N. Grid cell firing patterns signal environmental novelty by expansion. *Proc. Natl Acad. Sci. USA* **109**, 17687–17692 (2013).
80. Burgess, N., Barry, C. & O'Keefe, J. An oscillatory interference model of grid cell firing. *Hippocampus* **17**, 801–812 (2007).
81. Hasselmo, M. E., Giocomo, L. M. & Zilli, E. A. Grid cell firing may arise from interference of theta frequency membrane potential oscillations in single neurons. *Hippocampus* **17**, 1252–1271 (2007).
82. Blair, H. T., Weldon, A. C. & Zhang, K. Scale-invariant memory representations emerge from moire interference between grid fields that produce theta oscillations: a computational model. *J. Neurosci.* **27**, 3211–3229 (2007).
83. Giocomo, L. M., Moser, M.-B. & Moser, E. I. Computational models of grid cells. *Neuron* **71**, 589–603 (2011).
84. Little, W. A. The existence of persistent states in the brain. *Math. Biosci.* **19**, 101–120 (1971).
85. Hopfield, J. J. Neural networks and physical systems with emergent collective computational abilities. *Proc. Natl Acad. Sci. USA* **79**, 2554–2558 (1982).
86. Amit, D. J. *Modelling Brain Function: The World of Attractor Networks* (Cambridge Univ. Press, 1989).
87. Rolls, E. T. & Treves, A. *Neural Networks and Brain Function* (Oxford Univ. Press, 1998).
88. Hebb, D. O. *The Organization of Behavior* (Wiley, 1949).
89. Amari, S. Dynamics of pattern formation in lateral-inhibition type neural fields. *Biol. Cybern.* **27**, 77–87 (1977).
90. Lushajkin, A. V. & Georgopoulos, A. P. A dynamical neural network model for motor cortical activity during movement: population coding of movement trajectories. *Biol. Cybern.* **69**, 517–524 (1993).
91. Ben-Yishai, R., Bar-Or, R. L. & Sompolinsky, H. Theory of orientation tuning in visual cortex. *Proc. Natl Acad. Sci. USA* **92**, 3844–3848 (1995).
92. Sompolinsky, H. & Shapley, R. New perspectives on the mechanisms for orientation selectivity. *Curr. Opin. Neurobiol.* **7**, 514–522 (1997).
93. Seung, H. S. How the brain keeps the eyes still. *Proc. Natl Acad. Sci. USA* **95**, 13339–13344 (1996).
94. McNaughton, B. L., Chen, L. L. & Markus, E. J. "Dead reckoning", landmark learning, and the sense of direction: a neurophysiological and computational hypothesis. *J. Cogn. Neurosci.* **3**, 190–202 (1991).
95. Zhang, K. Representation of spatial orientation by the intrinsic dynamics of the head-direction cell ensemble: a theory. *J. Neurosci.* **16**, 2112–2126 (1996).
96. Tsodyks, M. & Sejnowski, T. Associative memory and hippocampal place cells. *Int. J. Neural Syst.* **6** (Suppl.), 81–86 (1995).
97. Samsonovich, A. & McNaughton, B. L. Path integration and cognitive mapping in a continuous attractor neural network model. *J. Neurosci.* **17**, 5900–5920 (1997).
98. Battaglia, F. P. & Treves, A. Attractor neural networks storing multiple space representations: a model for hippocampal place fields. *Phys. Rev. E* **58**, 7738–7753 (1998).
99. Tsodyks, M. Attractor neural network models of spatial maps in hippocampus. *Hippocampus* **9**, 481–489 (1999).
100. Fuhs, M. C. & Touretzky, D. S. A spin glass model of path integration in rat medial entorhinal cortex. *J. Neurosci.* **26**, 4266–4276 (2006). **Along with McNaughton *et al.* (reference 3), this paper is one of the first to propose attractor dynamics combined with directional translation of an activity pattern as the underlying mechanism of grid cell formation. As opposed to the toroidal Mexican hat-type connectivity of McNaughton *et al.* that leads to a single bump of activity, the model by Fuhs and Touretzky considered a connectivity that periodically became negative and positive at large-phase differences, leading to the formation of a grid-like pattern on the network.**
101. Burak, Y. & Fiete, I. R. Accurate path integration in continuous attractor network models of grid cells. *PLoS Comput. Biol.* **5**, e1000291 (2009). **The authors report the first computer simulation of an attractor network in which grid cells are generated through a Mexican hat-like all-inhibitory connectivity pattern.**
102. Guanella, A., Kiper, D. & Verschure, P. A model of grid cells based on a twisted torus topology. *Int. J. Neural Syst.* **17**, 231–240 (2007).
103. Boccara, C. N. *et al.* Grid cells in pre- and parasubiculum. *Nature Neurosci.* **13**, 987–994 (2010).
104. Domnisoru, C., Kinkhabwala, A. A. & Tank, D. W. Membrane potential dynamics of grid cells. *Nature* **495**, 199–204 (2013).
105. Schmidt-Hieber, C. & Häusser, M. Cellular mechanisms of spatial navigation in the medial entorhinal cortex. *Nature Neurosci.* **16**, 325–331 (2013). **Domnisoru *et al.* (reference 104) and Schmidt-Hieber and Häusser carried out intracellular recordings from entorhinal stellate cells in rats navigating a virtual environment. The two papers demonstrate that fluctuations in membrane potential associated with grid fields are not primarily linked to local theta rhythm, arguing against oscillatory interference models.**
106. Dhillon, A. & Jones, R. S. Laminar differences in recurrent excitatory transmission in the rat entorhinal cortex *in vitro*. *Neuroscience* **99**, 413–422 (2000).
107. Couey, J. J. *et al.* Recurrent inhibitory circuitry as a mechanism for grid formation. *Nature Neurosci.* **16**, 318–324 (2013). **A combination of intracellular recordings and optogenetics was used to show that the effective interaction between layer II stellate cells is purely inhibitory. It was also shown through simulations that a simple all-or-none inhibitory connectivity — in which cells with nearby phases inhibit each other to exactly the same extent, whereas those that are far apart are not coupled — is sufficient to generate grid cells.**
108. Pastoll, H., Solanka, L., van Rossum, M. C. & Nolan, M. F. Feedback inhibition enables theta-nested gamma oscillations and grid firing fields. *Neuron* **77**, 141–154 (2013).
109. Bonnevie, T. *et al.* Grid cells require excitatory drive from the hippocampus. *Nature Neurosci.* **16**, 309–317 (2013).
110. Brandon, M. P. *et al.* Reduction of theta rhythm dissociates grid cell spatial periodicity from directional tuning. *Science* **332**, 595–599 (2011).
111. Koenig, J., Linder, A. N., Leutgeb, J. K. & Leutgeb, S. The spatial periodicity of grid cells is not sustained during reduced theta oscillations. *Science* **332**, 592–595 (2011).
112. Ts'o, D. Y., Gilbert, C. D. & Wiesel, T. N. Relationships between horizontal interactions and functional architecture in cat striate cortex as revealed by cross-correlation analysis. *J. Neurosci.* **6**, 1160–1170 (1986).
113. Gilbert, C. D. & Wiesel, T. N. Columnar specificity of intrinsic horizontal and corticocortical connections in cat visual cortex. *J. Neurosci.* **9**, 2432–2442 (1989).
114. Bosking, W. H., Zhang, Y., Schofield, B. & Fitzpatrick, D. Orientation selectivity and the arrangement of horizontal connections in tree shrew striate cortex. *J. Neurosci.* **17**, 2112–2127 (1997).
115. Ko, H. *et al.* Functional specificity of local synaptic connections in neocortical networks. *Nature* **473**, 87–91 (2011).
116. Mhatre, H., Gorchetchnikov, A. & Grossberg, S. Grid cell hexagonal patterns formed by fast self-organized learning within entorhinal cortex. *Hippocampus* **22**, 320–334 (2012).
117. Grossberg, S. & Pilly, P. K. How entorhinal grid cells may learn multiple spatial scales from a dorsoventral gradient of cell response rates in a self-organizing map. *PLoS Comput. Biol.* **8**, e1002648 (2012).
118. Buetfering, C., Allen, K. & Monyer, H. Parvalbumin interneurons provide grid cell-driven recurrent inhibition in the medial entorhinal cortex. *Nature Neurosci.* **17**, 710–718 (2014).
119. Roudi, Y. & Moser, E. I. Grid cells in an inhibitory network. *Nature Neurosci.* **17**, 639–641 (2014).
120. Mathis, A., Herz, A. V. & Stemmler, M. B. Multiscale codes in the nervous system: the problem of noise correlations and the ambiguity of periodic scales. *Phys. Rev. E Stat. Nonlin. Soft Matter Phys.* **88**, 022713 (2013).
121. Dunn, B., Mørreunet, M. & Roudi, Y. Correlations and functional connections in a population of grid cells. [online]. <http://arxiv.org/abs/1405.0044> (2014).
122. Roudi, Y. & Hertz, J. Mean field theory for nonequilibrium network reconstruction. *Phys. Rev. Lett.* **106**, 048702 (2011).
123. Tocker, G. & Derdikman, D. Relation between spatial and temporal synchronization in MEC grid-cells. *Soc. Neurosci. Abstr.* **39**, 769.27 (2013).
124. Langston, R. F. *et al.* Development of the spatial representation system in the rat. *Science* **328**, 1576–1580 (2010).
125. Wills, T. J., Cacciuci, F., Burgess, N. & O'Keefe, J. Development of the hippocampal cognitive map in preweanling rats. *Science* **328**, 1573–1576 (2010).
126. Kropff, E. & Treves, A. The emergence of grid cells: intelligent design or just adaptation? *Hippocampus* **18**, 1256–1269 (2008). **This paper proposes the only model for grid cells that is not primarily based on path integration. Grids are formed through a self-organizing mechanism that combines Hebbian plasticity, feedforward spatially selective input and neuronal adaptation.**
127. Stensola, T., Stensola, H., Moser, M.-B. & Moser, E. I. Environmental constraints on grid cell orientation. *Soc. Neurosci. Abstr.* **39**, 769.15 (2013).
128. Si, B., Kropff, E. & Treves, A. Grid alignment in entorhinal cortex. *Biol. Cybern.* **106**, 483–506 (2012).
129. Stella, F., Si, B., Kropff, E. & Treves, A. Grid cells on the ball. *J. Stat. Mech.* P03013 (2013).
130. Stella, F., Si, B., Kropff, E. & Treves, A. Grid maps for spaceflight, anyone? They are for free! *Behav. Brain Sci.* **36**, 566–567 (2013).
131. Kruge, I. U., Wernle, T., Moser, E. I. & Moser, M.-B. Grid cells of animals raised in spherical environments. *Soc. Neurosci. Abstr.* **39**, 769.14 (2013).
132. Douglas, R. J. & Martin, K. A. Neuronal circuits of the neocortex. *Annu. Rev. Neurosci.* **27**, 419–451 (2004).
133. Lefort, S., Tomm, C., Floyd Sarria, J. C. & Petersen, C. C. The excitatory neuronal network of the C2 barrel column in mouse primary somatosensory cortex. *Neuron* **61**, 301–316 (2009).
134. McGuire, B. A., Gilbert, C. D., Rivlin, P. K. & Wiesel, T. N. Targets of horizontal connections in macaque primary visual cortex. *J. Comp. Neurol.* **305**, 370–392 (1991).
135. Binzegger, T., Douglas, R. J. & Martin, K. A. A quantitative map of the circuit of cat primary visual cortex. *J. Neurosci.* **24**, 8441–8453 (2004).

136. Haberly, L. B. & Presto, S. Ultrastructural analysis of synaptic relationships of intracellularly stained pyramidal cell axons in piriform cortex. *J. Comp. Neurol.* **248**, 464–474 (1986).
137. Miles, R. & Wong, R. K. Excitatory synaptic interactions between CA3 neurons in the guinea-pig hippocampus. *J. Physiol.* **373**, 397–418 (1986).
138. Ishizuka, N., Weber, J. & Amaral, D. G. Organization of intrahippocampal projections originating from CA3 pyramidal cells in the rat. *J. Comp. Neurol.* **295**, 580–623 (1990).
139. Li, X. G., Somogyi, P., Ylinen, A. & Buzsáki, G. The hippocampal CA3 network: an *in vivo* intracellular labeling study. *J. Comp. Neurol.* **339**, 181–208 (1994).
140. Harris, E., Witter, M. P., Weinstein, G. & Stewart, M. Intrinsic connectivity of the rat subiculum: I. dendritic morphology and patterns of axonal arborization by pyramidal neurons. *J. Comp. Neurol.* **435**, 490–505 (2001).
141. Funahashi, M. & Stewart, M. Presubicular and parasubicular cortical neurons of the rat: functional separation of deep and superficial neurons *in vitro*. *J. Physiol.* **501**, 387–403 (1997).
142. Wachowiak, M. & Shipley, M. T. Coding and synaptic processing of sensory information in the glomerular layer of the olfactory bulb. *Semin. Cell Dev. Biol.* **17**, 411–423 (2006).
143. Scharfman, H. E., Kunkel, D. D. & Schwartzkroin, P. A. Synaptic connections of dentate granule cells and hilar neurons: results of paired intracellular recordings and intracellular horseradish peroxidase injections. *Neuroscience* **37**, 693–707 (1990).
144. Acsády, L., Kamondi, A., Sik, A., Freund, T. & Buzsáki, G. GABAergic cells are the major postsynaptic targets of mossy fibers in the rat hippocampus. *J. Neurosci.* **18**, 3386–3403 (1998).
145. Jung, M. W. & McNaughton, B. L. Spatial selectivity of unit activity in the hippocampal granular layer. *Hippocampus* **3**, 165–182 (1993).
146. Leutgeb, J. K., Leutgeb, S., Moser, M.-B. & Moser, E. I. Pattern separation in the dentate gyrus and CA3 of the hippocampus. *Science* **315**, 961–966 (2007).
147. Spruston, N. & Johnston, D. Perforated patch-clamp analysis of the passive membrane properties of three classes of hippocampal neurons. *J. Neurophysiol.* **67**, 508–529 (1992).
148. Gatome, C. W., Slomianka, L., Lipp, H. P. & Amrein, I. Number estimates of neuronal phenotypes in layer II of the medial entorhinal cortex of rat and mouse. *Neuroscience* **170**, 156–165 (2010).
149. Steward, O. & Scoville, S. A. Cells of origin of entorhinal cortical afferents to the hippocampus and fascia dentata of the rat. *J. Comp. Neurol.* **169**, 347–370 (1976).
150. Tamamaki, N. & Nojyo, Y. Projection of the entorhinal layer II neurons in the rat as revealed by intracellular pressure-injection of neurobiotin. *Hippocampus* **3**, 471–480 (1993).
151. Zhang, S. J. *et al.* Optogenetic dissection of entorhinal-hippocampal functional connectivity. *Science* **340**, 1232627 (2013).
152. Dickson, C. T., Mena, A. R. & Alonso, A. Electroresponsiveness of medial entorhinal cortex layer III neurons *in vitro*. *Neuroscience* **81**, 937–950 (1997).
153. Hamam, B. N., Kennedy, T. E., Alonso, A. & Amaral, D. G. Morphological and electrophysiological characteristics of layer V neurons of the rat medial entorhinal cortex. *J. Comp. Neurol.* **418**, 457–472 (2000).
154. Leutgeb, S. *et al.* Independent codes for spatial and episodic memory in hippocampal neuronal ensembles. *Science* **309**, 619–623 (2005).
155. Jezek, K., Henriksen, E. J., Treves, A., Moser, E. I. & Moser, M.-B. Theta-paced flickering between place-cell maps in the hippocampus. *Nature* **478**, 246–249 (2011).
156. Hubel, D. H. & Wiesel, T. Receptive fields, binocular interaction, and functional architecture of cat striate cortex. *J. Physiol. (Lond.)* **160**, 106–154 (1962). **An extensive description of the striate cortex, including its columnar organization and receptive field properties. The authors propose a model of how the concentric circular ‘on or off’ receptive fields of retinal ganglion cells and geniculate neurons could combine to form linear receptive fields in the primary visual cortex. This model still has merit half a century later.**
157. O’Keefe, J. & Burgess, N. Dual phase and rate coding in hippocampal place cells: theoretical significance and relationship to entorhinal grid cells. *Hippocampus* **15**, 853–866 (2005).
158. Solstad, T., Moser, E. I. & Einfeldt, G. T. From grid cells to place cells: a mathematical model. *Hippocampus* **16**, 1026–1031 (2006).
159. Rolls, E. T., Stringer, S. M. & Elliot, T. Entorhinal cortex grid cells can map to hippocampal place cells by competitive learning. *Network* **17**, 447–465 (2006).
160. Savelli, F. & Knierim, J. J. Hebbian analysis of the transformation of medial entorhinal grid-cell inputs to hippocampal place fields. *J. Neurophysiol.* **103**, 3167–3183 (2010).
161. de Almedia, L., Idiart, M. & Lisman, J. E. The input-output transformation of the hippocampal granule cells: from grid cells to place cells. *J. Neurosci.* **29**, 7504–7512 (2009).
162. Monaco, J. D. & Abbott, L. F. Modular realignment of entorhinal grid cell activity as a basis for hippocampal remapping. *J. Neurosci.* **31**, 9414–9425 (2011).
163. O’Keefe, J. & Burgess, N. Geometric determinants of the place fields of hippocampal neurons. *Nature* **381**, 425–428 (1996).
164. Hartley, T., Burgess, N., Lever, C., Cacucci, F. & O’Keefe, J. Modeling place fields in terms of the cortical inputs to the hippocampus. *Hippocampus* **10**, 369–379 (2000).
165. O’Keefe, J. & Conway, D. H. Hippocampal place units in the freely moving rat: why they fire where they fire. *Exp. Brain Res.* **31**, 573–590 (1978).
166. Wiener, S. I., Paul, C. A. & Eichenbaum, H. Spatial and behavioral correlates of hippocampal neuronal activity. *J. Neurosci.* **9**, 2737–2763 (1989).
167. Hetherington, P. A. & Shapiro, M. L. Hippocampal place fields are altered by the removal of single visual cues in a distance-dependent manner. *Behav. Neurosci.* **111**, 20–34 (1997).
168. Bjerknes, T. L., Moser, E. I. & Moser, M.-B. Representation of geometric borders in the developing rat. *Neuron* **82**, 71–78 (2014).
169. Jia, H., Rochefort, N. L. & Konnerth, A. Dendritic organization of sensory input to cortical neurons *in vivo*. *Nature* **464**, 1307–1312 (2010).
170. Chen, T. W. *et al.* Ultrasensitive fluorescent proteins for imaging neuronal activity. *Nature* **499**, 295–300 (2013).
171. Singer, W. Synchronization of cortical activity and its putative role in information processing and learning. *Annu. Rev. Physiol.* **55**, 349–374 (1993).
172. Fries, P. Neuronal gamma-band synchronization as a fundamental process in cortical computation. *Annu. Rev. Neurosci.* **32**, 209–224 (2009).
173. Colgin, L. L. *et al.* Frequency of gamma oscillations routes flow of information in the hippocampus. *Nature* **462**, 353–357 (2009).
174. Igarashi, K. M., Lu, L., Colgin, L. L., Moser, M.-B. & Moser, E. I. Coordination of entorhinal–hippocampal ensemble activity during associative learning. *Nature* <http://dx.doi.org/10.1038/nature13162> (2014).
175. Ahmed, O. J. & Mehta, M. R. Running speed alters the frequency of hippocampal gamma oscillations. *J. Neurosci.* **32**, 7373–7383 (2012).
176. Springer, M. S., Stanhope, M. J., Madsen, O. & de Jong, W. W. Molecules consolidate the placental mammal tree. *Trends Ecol. Evol.* **19**, 430–438 (2004).
177. Rodríguez, F. *et al.* Spatial memory and hippocampal pallium through vertebrate evolution: insights from reptiles and teleost fish. *Brain Res. Bull.* **57**, 499–503 (2002).
178. López, J. C., Vargas, J. P., Gómez, Y. & Salas, C. B. Spatial and non-spatial learning in turtles: the role of medial cortex. *Behav. Brain Res.* **143**, 109–120 (2003).
179. Broglio, C., Rodríguez, F., Gómez, A., Arias, J. L. & Salas, C. Selective involvement of the goldfish lateral pallium in spatial memory. *Behav. Brain Res.* **210**, 191–201 (2010).
180. Sperry, R. W. Chemoaffinity in the orderly growth of nerve fiber patterns and connections. *Proc. Natl Acad. Sci. USA* **50**, 703–710 (1963).
181. Penfield, W. & Rasmussen, T. *The Cerebral Cortex of Man. A Clinical Study of Localization of Function* (Macmillan, 1950).
182. Woolsey, T. A. & van der Loos, H. The structural organization of layer IV in the somatosensory region (SI) of mouse cerebral cortex. The description of a cortical field composed of discrete cytoarchitectonic units. *Brain Res.* **17**, 205–242 (1970).
183. Katsuki, Y., Sumi, T., Uchiyama, H. & Watanabe, T. Electrical responses of auditory neurons in cat to sound stimulation. *J. Neurophysiol.* **21**, 569–588 (1958).
184. Evans, E. F., Ross, H. F. & Whitfield, I. C. The spatial distribution of unit characteristic frequency in the primary auditory cortex of the cat. *J. Physiol. (Lond.)* **179**, 238–247 (1965).
185. Hubel, D. H. & Wiesel, T. Sequence regularity and geometry of orientation columns in the monkey striate cortex. *J. Comp. Neurol.* **158**, 267–294 (1974).
186. Blasdel, G. G. & Salama, G. Voltage sensitive dyes reveal a modular organization in monkey striate cortex. *Nature* **321**, 579–585 (1986).
187. Mooser, F., Bosking, W. H. & Fitzpatrick, D. A morphological basis for orientation tuning in primary visual cortex. *Nature Neurosci.* **7**, 872–879 (2004).
188. Gross, C. G., Bender, D. B. & Rocha-Miranda, C. E. Visual receptive fields of neurons in inferotemporal cortex of the monkey. *Science* **166**, 1303–1306 (1969).
189. Gross, C. G., Rocha-Miranda, C. E. & Bender, D. B. Visual properties of neurons in inferotemporal cortex of the macaque. *J. Neurophysiol.* **35**, 96–111 (1972).
190. Tanaka, K., Saito, H., Fukada, Y. & Moriya, M. Coding visual images of objects in the inferotemporal cortex of the macaque monkey. *J. Neurophysiol.* **66**, 170–189 (1991).
191. Bruce, C., Desimone, R. & Gross, C. G. Visual properties of neurons in a polysensory area in superior temporal sulcus in the macaque. *J. Neurophysiol.* **46**, 369–384 (1981).
192. Perrett, D. I., Rolls, E. T. & Caan, W. Visual neurones responsive to faces in the monkey temporal cortex. *Exp. Brain Res.* **47**, 329–342 (1982).
193. Rolls, E. Y. Neurons in the cortex of the temporal lobe and in the amygdala of the monkey with responses selective for faces. *Hum. Neurobiol.* **3**, 209–222 (1984).
194. Fujita, I., Tanaka, K., Ito, M. & Cheng, K. Columns for visual features of objects in monkey inferotemporal cortex. *Nature* **360**, 343–346 (1992).
195. Tsao, D. Y., Freiwald, W. A., Tootell, R. B. & Livingstone, M. S. A cortical region consisting entirely of face-selective cells. *Science* **311**, 670–674 (2006).
196. Tsao, D. Y., Moeller, S. & Freiwald, W. A. Comparing face patch systems in macaques and humans. *Proc. Natl Acad. Sci. USA* **105**, 19514–19519 (2008).
197. Moeller, S., Freiwald, W. A. & Tsao, D. Y. Patches with links: a unified system for processing faces in the macaque temporal lobe. *Science* **320**, 1355–1359 (2008).
198. Knudsen, E. I. & Konishi, M. A neural map of auditory space in the owl. *Science* **200**, 795–797 (1978).
199. Knudsen, E. I. & Konishi, M. Mechanisms of sound localization in the barn owl (*Tyto alba*). *J. Comp. Physiol.* **133**, 13–21 (1979).
200. Papp, E. A., Leergaard, T. B., Calabrese, E., Johnson, G. A. & Bjaalie, J. G. Waxholm Space atlas of the Sprague Dawley rat brain. *Neuroimage* **97**, 374–386 (2014).
201. Renart, A., Song, P. & Wang, X. J. Robust spatial working memory through homeostatic synaptic scaling in heterogeneous cortical networks. *Neuron* **38**, 473–485 (2003).
202. Roudi, Y. & Treves, A. Representing where along with what information in a model of a cortical patch. *PLoS Comput. Biol.* **4**, e1000012 (2007).
203. Itskov, V., Hansel, D. & Tsodyks, M. Short-term facilitation may stabilize parametric working memory trace. *Front. Comput. Neurosci.* **5**, 40 (2011).
204. Remme, M. W., Lengyel, M. & Gutkin, B. S. Democracy-independence trade-off in oscillating dendrites and its implications for grid cells. *Neuron* **66**, 429–437 (2010).
205. Burgess, N. Grid cells and theta as oscillatory interference: theory and predictions. *Hippocampus* **18**, 1157–1174 (2008).
206. Zilli, E. A. & Hasselmo, M. E. Coupled noisy spiking neurons as velocity-controlled oscillators in a model of grid cell spatial firing. *J. Neurosci.* **30**, 13850–13860 (2010).
207. Hafting, T., Fyhn, M., Bonnevie, T., Moser, M.-B. & Moser, E. I. Hippocampus-independent phase precession in entorhinal grid cells. *Nature* **453**, 1248–1252 (2008).
208. Navratilova, Z., Giocomo, L. M., Fellous, J. M., Hasselmo, M. E. & McNaughton, B. L. Phase precession and variable spatial scaling in a periodic attractor map model of medial entorhinal grid cells with realistic after-spike dynamics. *Hippocampus* **22**, 772–789 (2012).
209. Heys, J. G., MacLeod, K. M., Moss, C. F. & Hasselmo, M. E. Bat and rat neurons differ in theta-frequency resonance despite similar coding of space. *Science* **340**, 363–367 (2013).

210. Giocomo, L. M. & Hasselmo, M. E. Knock-out of HCN1 subunit flattens dorsal-ventral frequency gradient of medial entorhinal neurons in adult mice. *J. Neurosci.* **29**, 7625–7630 (2009).
211. Giocomo, L. M. *et al.* Grid cells use HCN1 channels for spatial scaling. *Cell* **147**, 1159–1170 (2011).
212. Bush, D. & Burgess, N. A hybrid oscillatory interference/continuous attractor network model of grid cell firing. *J. Neurosci.* **34**, 5065–5079 (2014).
213. Barry, C. & Doeller, C. F. 3D mapping in the brain. *Science* **340**, 279–280 (2013).
214. Hasselmo, M. E. & Brandon, M. P. A model combining oscillations and attractor dynamics for generation of grid cell firing. *Front. Neural Circuits* **6**, 30 (2012).
215. Yasuda, M. & Mayford, M. R. CaMKII activation in the entorhinal cortex disrupts previously encoded spatial memory. *Neuron* **50**, 309–318 (2006).
216. Fenno, L., Yizhar, O. & Deisseroth, K. The development and application of optogenetics. *Annu. Rev. Neurosci.* **34**, 389–412 (2011).
217. Alexander, G. M. *et al.* Remote control of neuronal activity in transgenic mice expressing evolved G protein-coupled receptors. *Neuron* **63**, 27–39 (2009).
218. Miyawaki, A. *et al.* Fluorescent indicators for Ca<sup>2+</sup> based on green fluorescent proteins and calmodulin. *Nature* **388**, 882–887 (1997).
219. Miyawaki, A., Griesbeck, O., Heim, R. & Tsien, R. Y. Dynamic and quantitative Ca<sup>2+</sup> measurements using improved cameleons. *Proc. Natl Acad. Sci. USA* **96**, 2135–2140 (1999).
220. Heim, N. *et al.* Improved calcium imaging in transgenic mice expressing a troponin C-based biosensor. *Nature Methods* **4**, 127–129 (2007).
221. Mank, M. *et al.* A genetically encoded calcium indicator for chronic *in vivo* two-photon imaging. *Nature Methods* **5**, 805–811 (2008).
222. Tian, L. *et al.* Imaging neural activity in worms, flies and mice with improved GCaMP calcium indicators. *Nature Methods* **6**, 875–881 (2009).
223. Looger, L. L. & Griesbeck, O. Genetically encoded neural activity indicators. *Curr. Opin. Neurobiol.* **22**, 18–23 (2012).
224. Harvey, C. D., Collman, F., Dombeck, D. A. & Tank, D. W. Intracellular dynamics of hippocampal place cells during virtual navigation. *Nature* **461**, 941–946 (2009).
225. Taniguchi, H. *et al.* A resource of Cre driver lines for genetic targeting of GABAergic neurons in cerebral cortex. *Neuron* **71**, 995–1013 (2011).
226. Girardeau, G., Benchenane, K., Wiener, S. I., Buzsáki, G. & Zugaro, M. B. Selective suppression of hippocampal ripples impairs spatial memory. *Nature Neurosci.* **12**, 1222–1223 (2009).
227. Wickersham, I. R. *et al.* Monosynaptic restriction of transsynaptic tracing from single, genetically targeted neurons. *Neuron* **53**, 639–647 (2007).
228. Wickersham, I. R., Finke, S., Conzelmann, K. K. & Callaway, E. M. Retrograde neuronal tracing with a deletion-mutant rabies virus. *Nature Methods* **4**, 47–49 (2007).
229. Moser, E. I. & Moser, M.-B. Grid cells and neural coding in high-end cortices. *Neuron* **80**, 765–774 (2013).

#### Acknowledgements

The authors are grateful to T. Mrsic-Flogel for comments on the manuscript. The authors thank the European Research Council ('CIRCUIT' Advanced Investigator Grant, grant agreement 232608; 'ENSEMBLE' Advanced Investigator Grant, grant agreement 268598), the European Commission's FP7 FET Proactive programme on Neuro-Bio-Inspired Systems (grant agreement 600725), an FP7 Marie Curie Training Network Grant (NETADIS; grant agreement 290038), the Louis-Jeantet Prize for Medicine, the Kavli Foundation and the Centre of Excellence scheme and the FRIPRO and NEVRONOR programmes of the Research Council of Norway for support. The authors thank T. Stensola for the design of figure 1 parts b and d. The authors are also grateful to F. Pinheiro for suggesting the Borges quote.

#### Competing interests statement

The authors declare no competing interests.